

Chapter 4

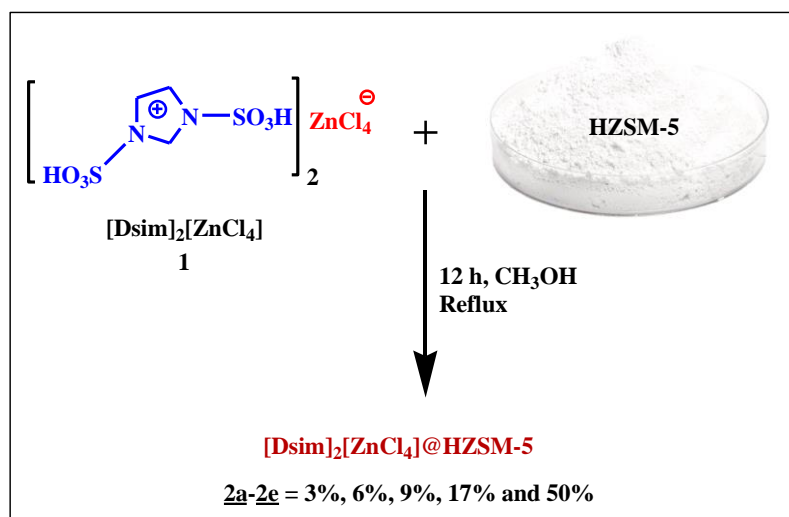
Design of dual acidic 1, 3-disulfoimidazolium chlorozincate supported HZSM-5 materials and their catalytic use in the synthesis of indole derivatives

Published with modification

Saikia, S., Puri, K. and Borah, R. Supported dual-acidic 1, 3-disulfoimidazolium chlorozincate@HZSM-5 as a promising heterogeneous catalyst for synthesis of indole derivatives. *Applied Organometallic Chemistry*, 33(3):1-12, 2019.

4A.1 Introduction

Hybrid material obtained *via* immobilization of acidic chlorometallates on ZSM-5 support combines various properties of zeolites like solid acidity, shape selectivity, porosity, crystallinity and high surface area with task-specific nature of the chlorometallate salts, leads to formation of structurally modified framework of the zeolite material with uniform distribution of active sites of the ionic salt on its surface. As mentioned in **Section 3A** (subunit **3A.2**, **Chapter 3**), structural change of siliceous ammoniated ZSM-5 zeolite occurs at 500°C during conversion to acidic HZSM-5 through thermal initiated dealumination process [1]. Then the dealuminated HZSM-5 structure can be remodified upon treatment with suitable acidic material involving realumination of extraframework Al species to the zeolite network. High content of Si/Al ratio is retained in the modified hybrid material of the siliceous HZSM-5 framework with slight loss of crystallinity as compared to parent HZSM-5. These structural changes also effect on micropore sizes of the zeolites which can be easily investigated using N₂ adsorption-desorption isotherm. Also, greater silica content makes ZSM-5 less prone towards dealumination which has been proved as common problem for low silica zeolites during immobilization of acidic materials. Details on chlorometallate discussed in **Chapter 1** and **Chapter 2 (Section 2A)** revealed their structural behaviors, advantages as well as related disadvantages. Despite having different functionalities, they have been suffering from drawbacks like water sensitivity, low thermal stability *etc.* The idea of immobilization or support on ZSM-5 offers a scope to turn their drawbacks into advantages by increasing water stability along with thermal stability. Also, this concept can be utilized to combine certain specific nature of the metal containing ionic solid (e.g. Brönsted/Lewis acidity, magnetic properties, fluorescence *etc.*) with unique properties of the zeolite support for efficient applications as solid acidic composites [2]. Herein, we aimed to immobilize known [3] Brönsted-Lewis acidic 1, 3-disulfoimidazolium chlorozincate ([Dsim]₂[ZnCl₄]) ionic salt on HZSM-5 support in different w/w ratios (3%, 6%, 9% 17% and 50%) by wet impregnation method according to **Scheme 4A.1** [4] and studied their catalytic activities for one-pot Fischer indole synthesis in solvent-free thermal treatment with various ketones.



Scheme 4A.1: Synthesis of $[\text{Dsim}]_2[\text{ZnCl}_4]@\text{HZSM-5}$

4A.2 Biological importance of indole derivatives

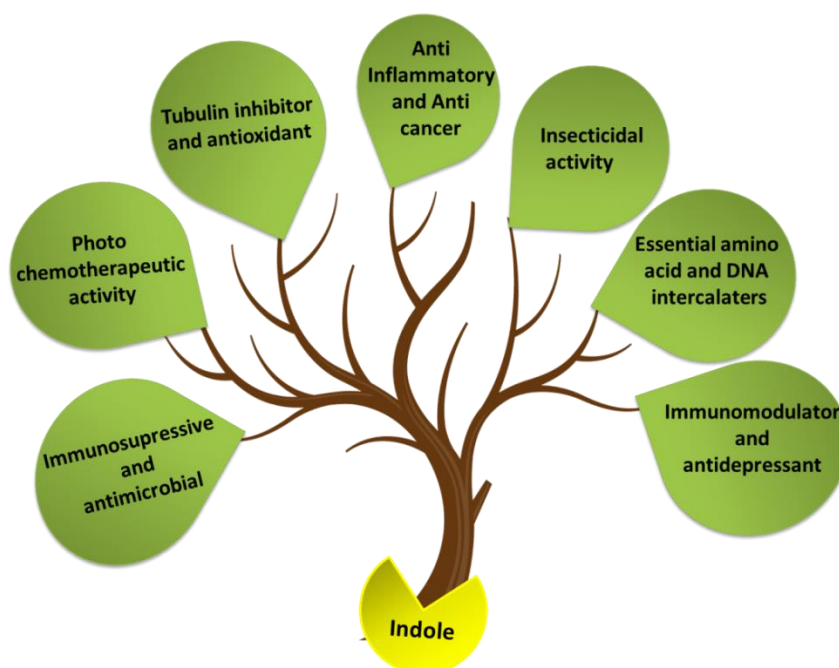


Fig.4A.1: Importance of indoles

Organic and medicinal chemists have been exploring heterocyclic chemistry way too extensively and proved the true utility of heterocycles as core scaffold of various medicinally active compounds and variety of polycyclic frameworks with the most diverse physical, chemical and biological properties. The combination of special polycyclic structures results in attractive and highly functionalized biologically active compounds. Among the broad range of heterocyclic compounds, indoles play a

significant role in biochemical processes of life as well as many other chemical processes. Intrinsic behavior of indoles relates similarly to the other heterocycles which are essential building blocks of many amino acids and in turn becomes integral part of enzyme and coenzyme actions in body. Apart from these, indoles have various clinical and other biological properties. Some indole derivatives occur naturally and others can be synthesized which act differently to pursue various actions related to human being (Fig. 4A.1).

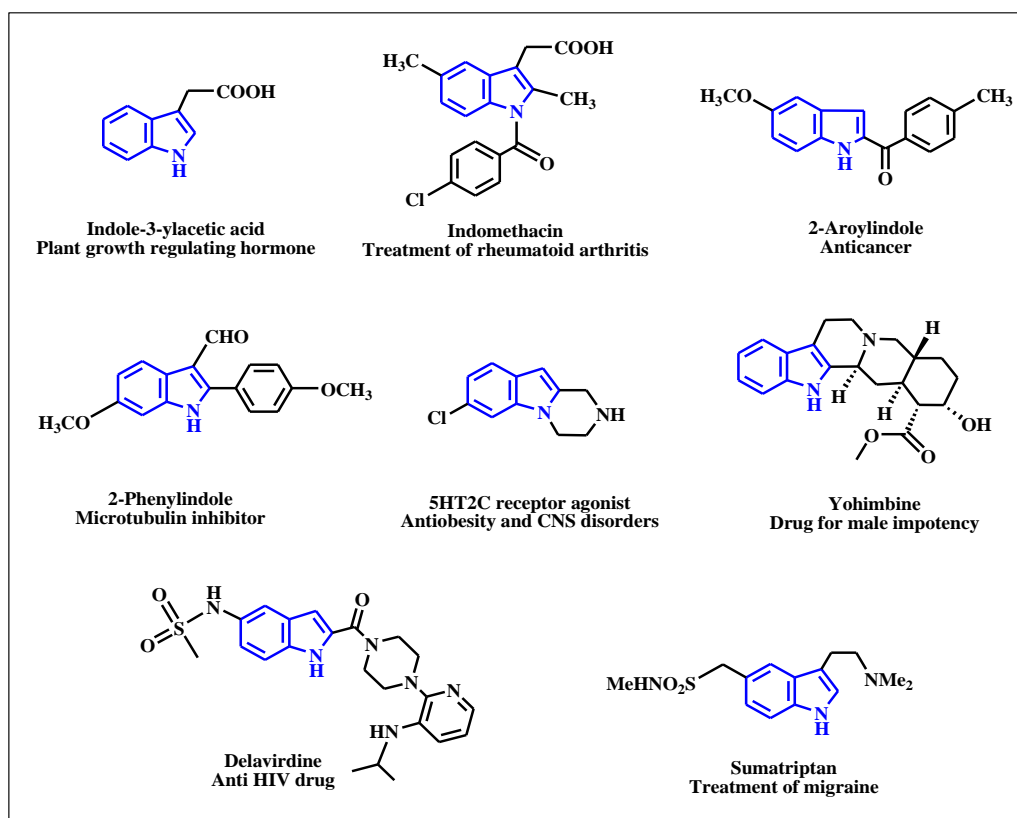


Fig.4A.2: Some examples of biologically active indole derivatives

Fig.4A.2 depicts some examples of important indole derivatives having pharmacological and biological significance [5]. There are innumerable indole based drug molecules available till date. It is somewhat difficult to embrace all the indole derivatives having medicinal or other activities in this small space.

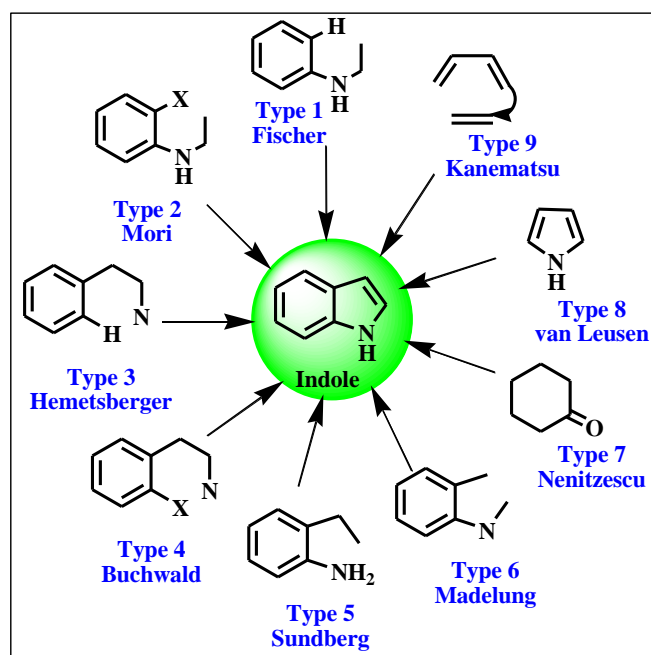


Fig.4A.3: Classification of indole synthesis

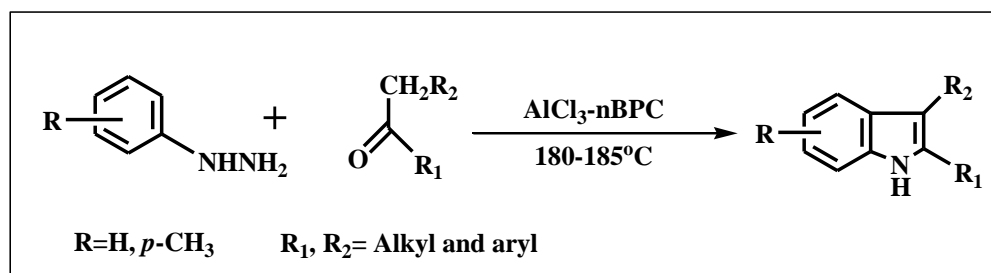
Taber *et al.* proposed the classification of indole synthesis based on construction patterns as shown in **Fig.4A.3** [6]. The authors differentiated nine types of indole synthesis and pointed out the difference between them. They distinguished Type 1 from Type 2 and Type 3 from Type 4, through forming a bond to a functionalized aromatic carbon, and also forming a bond to an aromatic carbon occupied only by a proton. Type 5 includes C-N bond formation as the last step whereas Type 6 has C-C bond formation as the last step. The benzene ring has been derived from an existing cyclohexane in Type 7 while in Type 8, the benzene ring has been built onto an existing pyrrole and lastly, in Type 9, both rings have been constructed. The author mentioned almost all the name reactions related to various types of indole synthesis and included in the **Fig.4A.3**. Some of these name reactions are Bartoli indole synthesis (Type 1), Bischler indole synthesis (Type 5), Fischer indole synthesis (Type 1), Hemetsberger indole synthesis (Type 3), Julia indole synthesis (Type 5), Larock indole synthesis (Type 5), Leimgruber-Batcho indole synthesis (Type 5), Madelung indole synthesis (Type 6), Nenitzescu indole synthesis (Type 7), Reissert indole synthesis (Type 5), Sundberg indole synthesis (Type 5) *etc.* Among them Fischer indole synthesis is one of the most widely studied method for the synthesis of indoles.

4A.3 Fischer indole synthesis

The Fischer indole synthesis was discovered in 1883 by Emil Fischer. It involves elimination of ammonia from arylhydrazone of an aldehyde or ketone, by treatment with an acid or various metal and anhydrous metal salt catalysts, with formation of an indole nucleus. In 1962, Robinson published a thorough study on the Fischer indole synthesis and mentioned all possible steps related to the mechanism of Fischer indole synthesis [7]. Also the author reviewed the role of catalysis in this synthesis. This review summarized a large number of catalysts such as various concentrated and dilute acids and acid mixtures (H_2SO_4 , HCl), metals and metal halides (Cu, Co, Ni, Zn, Mg *etc.*), Grignard reagents (PhMgBr, EtMgBr *etc.*), other acids (polyphosphoric acid, formic acid, acetic acid *etc.*) and many more. Study revealed the limitations of these catalysts such as low yield, large quantity of catalyst, hazardous materials, handling difficulty and sometimes only black intractable tars are obtained as dehydrogenation products. Simultaneous dehydrogenation is a major disadvantage of these catalysts. Besides the wide variety of Brønsted [8-11], Lewis [12-14] and solid acid (zeolite, clay) [15-17] catalysts, some noncatalytic indolization has also been reported in high temperature aqueous media [18] as well as in different solvents [19] like ethylene glycol, diethylene glycol, and tetralin. All these methods suffered several drawbacks when undergoing cyclization of arylhydrazone to indole. To eliminate some of the above mentioned disadvantages of Fischer indole reaction, ionic liquids have been utilized as solvent or dual solvent/catalyst systems. The next section covers the published works of Fischer indole reaction till 2017 involving ionic liquid as medium or dual functionalized solvent/catalyst system.

4A.4 Ionic liquids in Fischer indole synthesis

In 2001, Rebeiro *et al.* utilized 1-butylpyridinium chloride- AlCl_3 (n-BPC- AlCl_3) as dual solvent-catalyst system with an apparent mole ratio of 23:67 for the Fischer indole synthesis of both cyclic and acyclic ketones (**Scheme 4A.2**) [20]. The reaction involved stirring of various phenyl hydrazine derivatives and ketones at 180-185°C in presence of slight excess of ionic liquid under N_2 atmosphere for 30 min to 3 hour reaction to form 41-92% yields of products.



Scheme 4A.2: Fischer indole synthesis reported by Rebeiro *et al.*

Morales and his group (2004) used another chlorometallate ionic liquid choline chloride.2ZnCl₂ (Ch⁺Zn₂Cl₅⁻) (**Fig.4A.4**) to synthesize 2, 3-disubstituted indoles by reaction of alkyl methyl ketones with different hydrazines and the products readily sublimed directly from the ionic liquid [21]. High yield of products was observed up to 88% in 1-4 h time frame at 95-120°C.

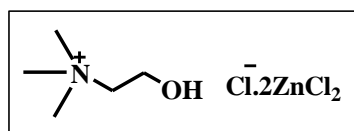


Fig.4A.4: Structure of choline chloride.2ZnCl₂

In the year 2007, Xu *et al.* employed a series of Brönsted acidic ionic liquids (BAILs) and tested their efficiency as dual solvent-catalysts in the indole synthesis (**Fig.4A.5**). Exclusive formation of 2, 3-disubstituted indoles was observed in the reaction of alkyl methyl unsymmetrical ketones yielding 83-97% of products after reaction in easily recyclable [BMIm][HSO₄] at 70-110°C in 0.5-6 h [22].

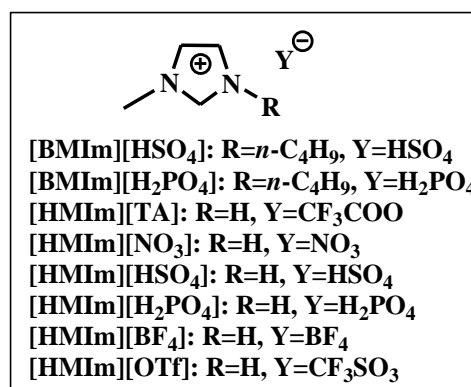
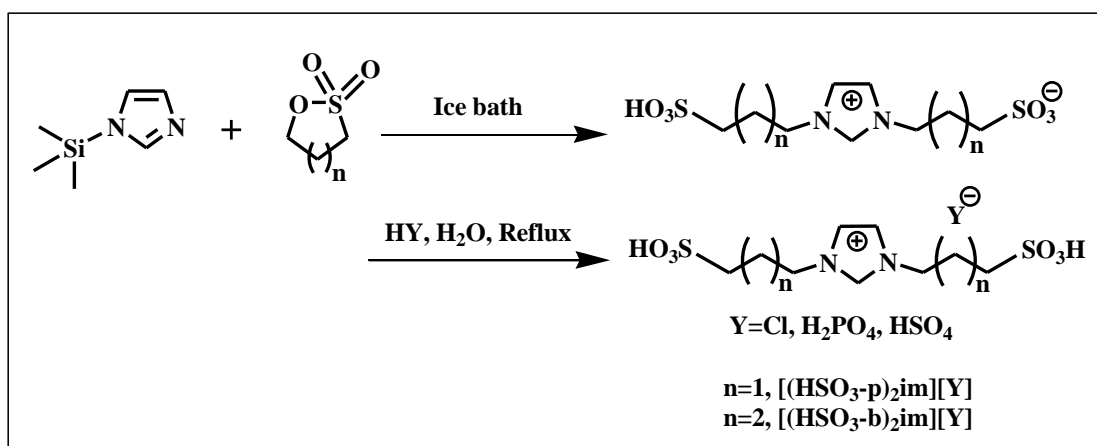
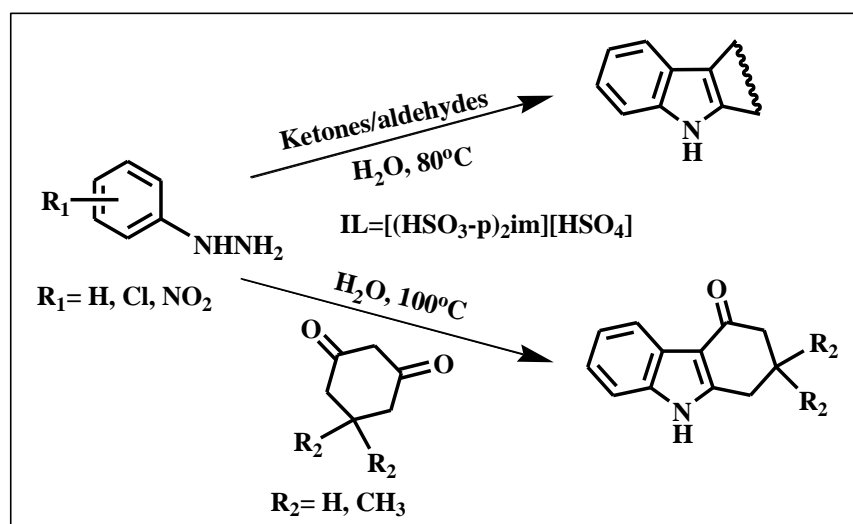


Fig.4A.5: Structure of Brönsted acidic ionic liquids

They also designed -SO₃H-functionalized ionic liquids bearing two alkyl sulfonic acid groups in the imidazolium cations (**Scheme 4A.3a**) and successfully performed their catalytic activity in water mediated Fischer indole synthesis. The reaction was extended to other types of indoles from single-carbonyl ketones/aldehydes (at 80°C) and cyclohexandiones (at 100°C) with 68-96% yields using the catalytic system of [(HSO₃-p)₂im][HSO₄]/H₂O [23] (**Scheme 4A.3b**). All the synthesized ionic liquids were screened for Hammett acidity. This method offered easy isolation of products as well as restoring of catalyst efficiently.



Scheme 4A.3a: Brønsted acidic ILs bearing two alkyl sulfonic acid groups



Scheme 4A.3b: Preparation of indoles using -N alkylsulfonic acid IL catalyst

In 2012, the same group used another reusable SO₃H-functionalized IL catalyst [(HSO₃-p)₂im][CF₃SO₃] (**Fig.4A.6**) for the preparation of indoles (86-96% of yields) from single-

carbonyl ketones/aldehydes or cyclohexanediones with arylhydrazine hydrochlorides in water under microwave irradiation at 100°C for 15-20 min [24]. They also compared the activity of this catalyst with other ionic liquids bearing similar cation but different anions like Cl^- , H_2PO_4^- , HSO_4^- and with their parent acids.

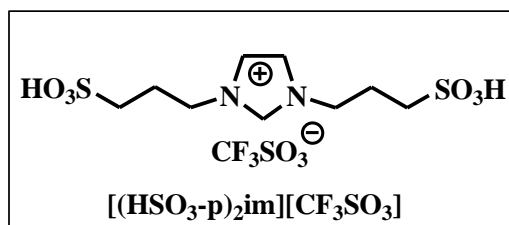


Fig.4A.6: Structure of $[(\text{HSO}_3\text{-p})_2\text{im}][\text{CF}_3\text{SO}_3]$

The catalytic activity of -COOH functionalized ionic liquid, 1-carboxymethyl-3-methylimidazolium tetrafluoroborate ($[\text{cmmim}][\text{BF}_4]$) (**Fig.4A.7**) was explored by Yi *et al.* for cyclization of phenyl hydrazine with cyclic/acyclic ketones at 130-150°C for 2 hours to produce 80-92% yields of the products [25]. The catalyst was efficiently reused for five cycles.

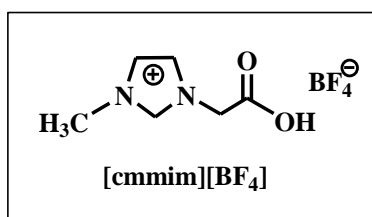
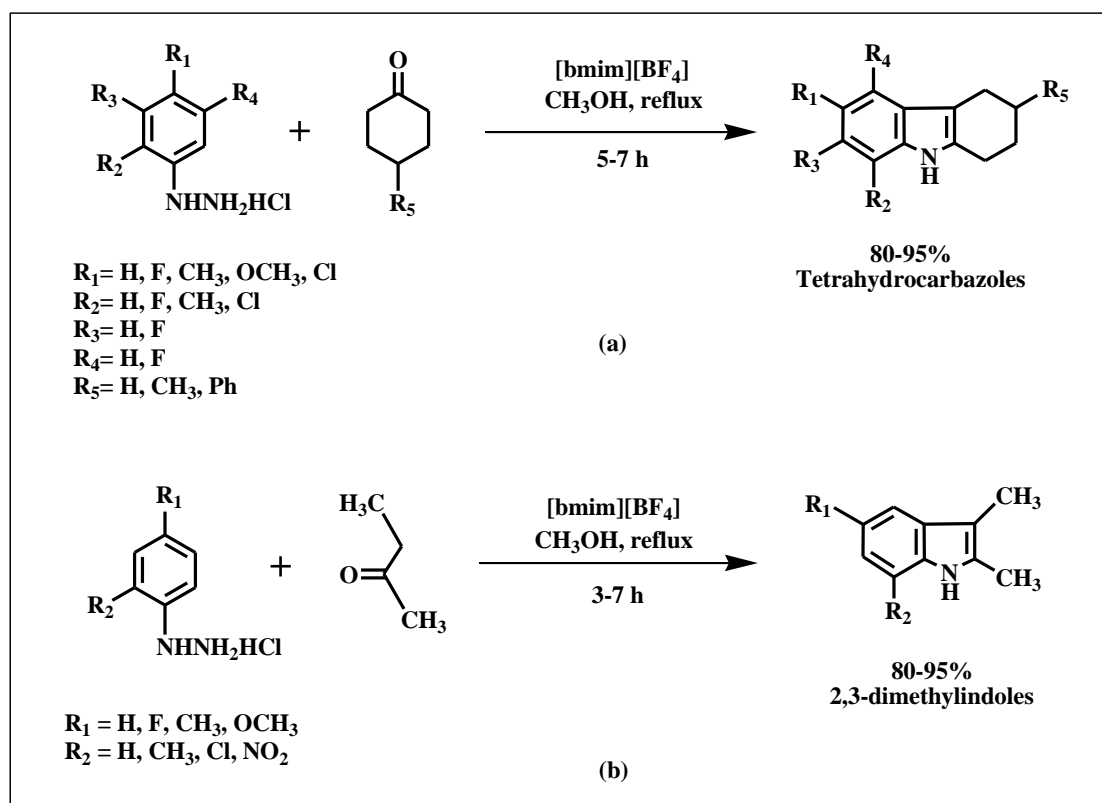


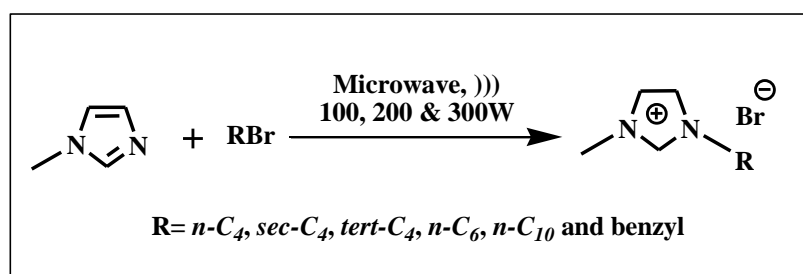
Fig.4A.7: Structure of $[\text{cmmim}][\text{BF}_4]$

Kumar *et al.* (2013) synthesized tetrahydrocarbazoles and 2, 3-dimethylindoles in methanol under reflux temperature using catalytic amount of reusable $[\text{bmim}][\text{BF}_4]$ ionic liquid for 3-7 hour reaction (**Scheme 4A.4**) [26].



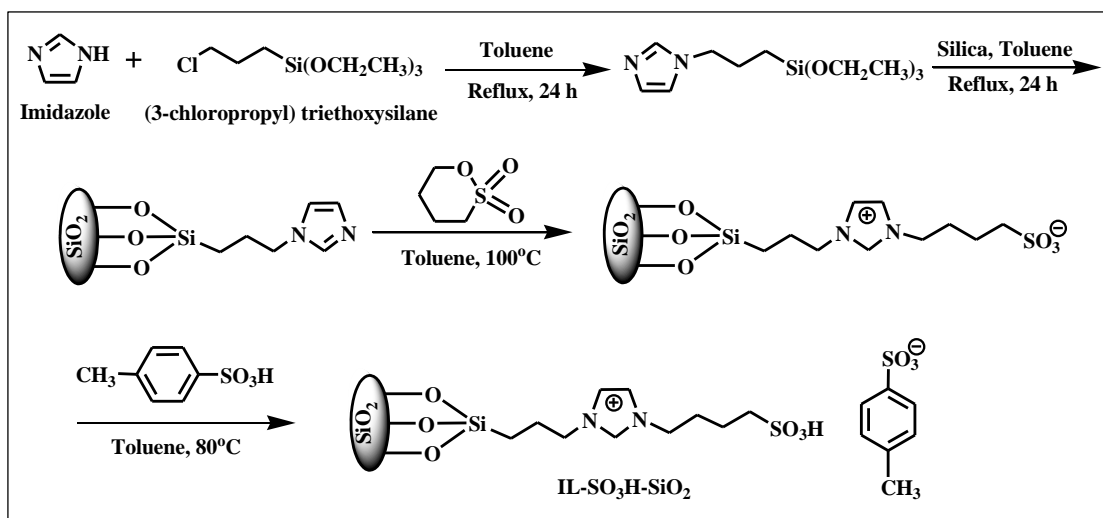
Scheme 4A.4: (a) Synthesis of tetrahydrocarbazole derivatives and (b) synthesis of 2, 3-dimethyl indole derivatives

Librando *et al.* (2015) synthesized a series of 1, 3-dialkylimidazolium bromide ILs using 1-methylimidazole and various alkyl bromides (**Scheme 4A.5**) [27]. They examined the catalytic ability of these ILs in microwave assisted Fischer indole synthesis of tetrahydrocarbazoles and compared with other catalytic systems like ionic liquid with ZnCl_2 and ZnCl_2 only. Among all the synthesized ionic liquids, the best performance was showed by 1-decyl-3-methylimidazolium bromide with ZnCl_2 (94% yield).

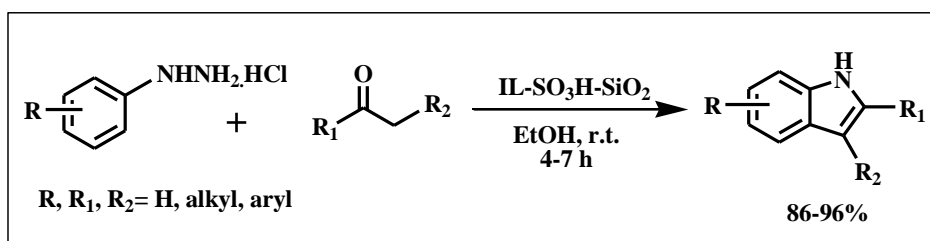


Scheme 4A.5: Synthesis of 1, 3-dialkylimidazolium bromide ILs

A silica gel supported functionalized ionic liquid active species 4-methylbenzenesulfonic acid (ILSO₃H-SiO₂) was developed by Hu *et al.* (**Scheme 4A.6a**) as an efficient heterogeneous catalyst for the synthesis of indoles at room temperature (**Scheme 4A.6b**) [28]. This method introduced mild reaction conditions, simplicity of operation, high yields, easy isolation of products, and excellent recyclability of the catalyst.

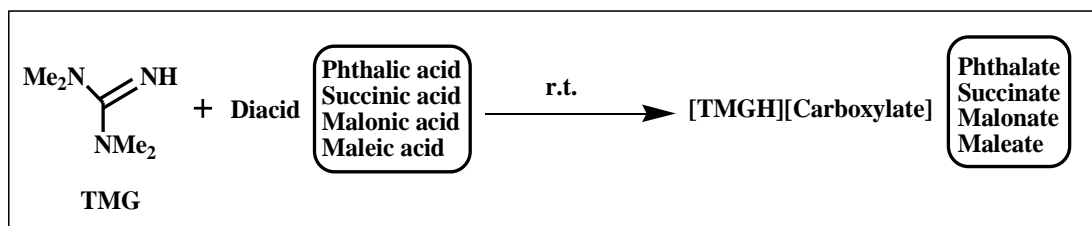


Scheme 4A.6a: Synthesis of supported ILSO₃H-SiO₂

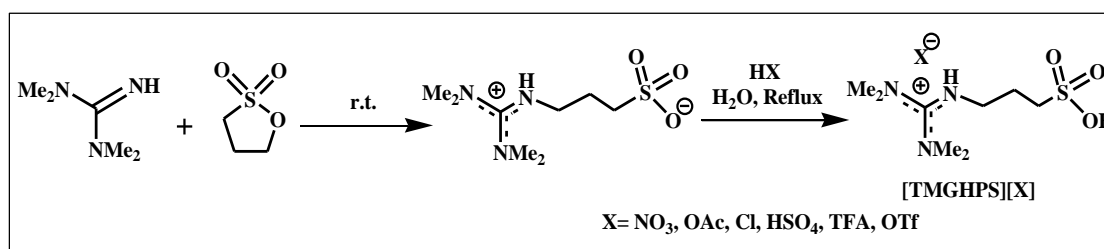


Scheme 4A.6b: Fischer indole synthesis catalyzed by ILSO₃H-SiO₂

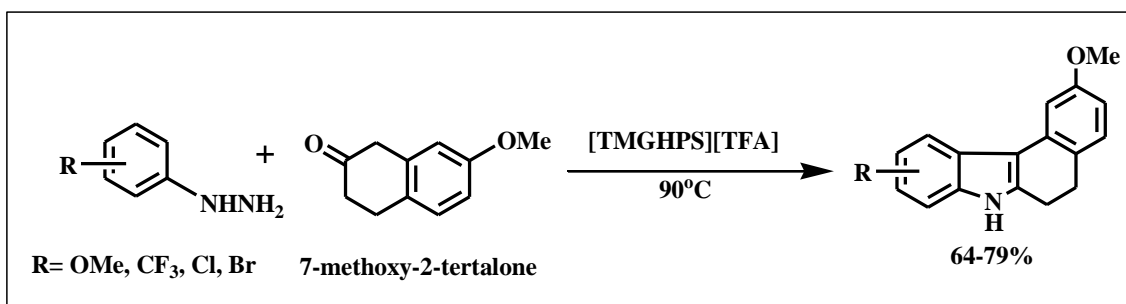
Two series of biodegradable protic ILs i.e. [TMGH]-carboxylate and TMG-sulfonic acid (**Scheme 4A.7a & 7b**) were prepared by Neuhaus *et al.* (2016) [29] and screened as solvent/catalyst at 90°C for the preparation of indoles with different ketones. They obtained tetramethylguanidinium propanesulfonic acid trifluoromethylacetate ([TMGHPS][TFA]) as the best reusable solvent/catalytic system for the indoles synthesis. Also, it satisfactorily catalyzed the synthesis of indoles from 7-methoxy-2-tetralones toward alkaloid core (**Scheme 4A.7c**).



Scheme 4A.7a: Synthesis of [TMGH][Carboxylate]

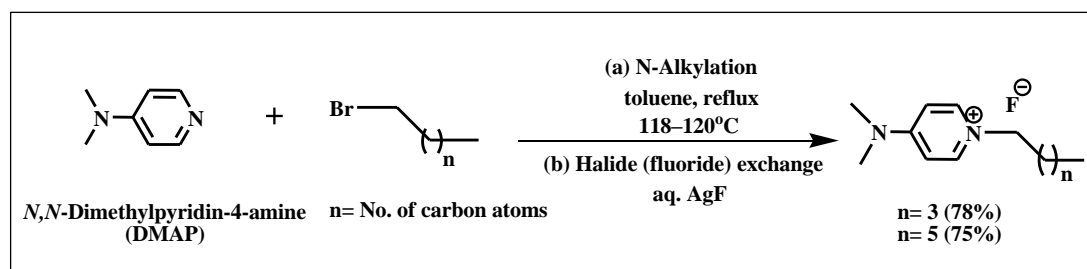


Scheme 4A.7b: Synthesis of [TMGHPS][X] ionic liquids



Scheme 4A.7c: Synthesis of indoles from 7-methoxy-2-tetralones toward alkaloid core

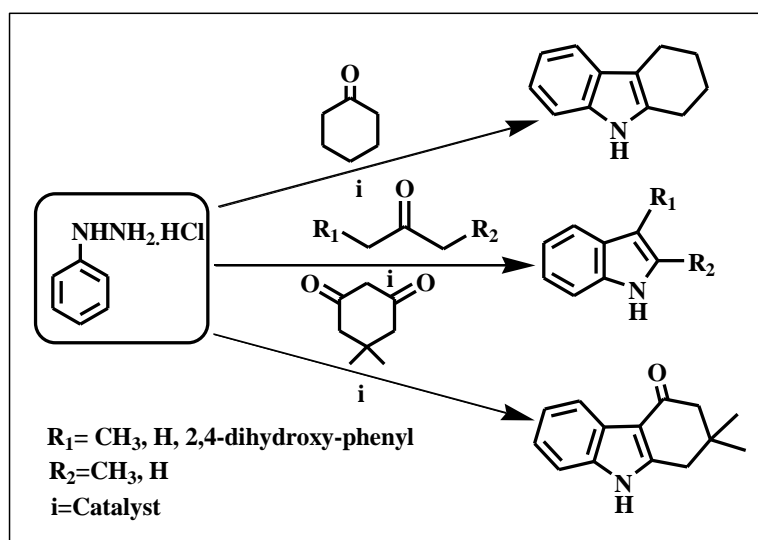
Recently, Ghumro *et al.* (2017) reported the preparation of two N, N-dimethylpyridin-4-amine (DMAP) based ionic liquids (ILs) (Scheme 4A.8) as efficient catalysts for the Fischer indole synthesis [30]. High thermal stability of the two ionic liquids facilitate them with added advantage of low toxicity than pyridine and also easy separation from the reaction mixture offered good yields of products up to 89% in ethanol at 78-80°C.



Scheme 4A.8: Synthesis of DMAP based ionic liquids

Yu *et al.* (2017) employed [emim][BF₄] ionic liquid as solvent in continuous flow Fischer indole synthesis of 3-methylindole by reaction of phenyl hydrazines and propylaldehyde in presence of stoichiometric Lewis acid, ZnCl₂ as catalyst [31].

Above discussion gave us the point to notice that there are not many ionic liquids involved in the Fischer indole synthesis. Also, there is only one or two ionic liquid based heterogeneous catalytic system reported till date. From the brief literature survey, it comes to light that catalytic system with advantages of ionic liquid and heterogeneous materials could bring new insights in the Fischer indole methodology. Therefore, keeping that in mind, we have developed a better method involving Lewis-Brønsted acidic 1, 3-disulfoimidazolium chlorozincate supported ZSM-5 materials as catalyst in the Fischer indole synthesis of phenyl hydrazine with various ketones (**Scheme 4A.9**). The results are mentioned in **Section 4B** of this chapter.



Scheme 4A.9: Fischer indole reaction

4B.1 Characterization of HZSM-5 supported ionic salts

This section proceeds with characterization of five [Dsim]₂[ZnCl₄]@HZSM-5 composites (w/w ratios 3%, 6%, 9% 17% and 50%) via various analytical techniques which include FT-IR, thermogravimetric analysis, powder-XRD, Raman, SEM, EDX, Hammett acidity and Lewis acidity determination, electronic spectra, BET-analysis, ICP-OES techniques *etc.* Physicochemical nature of the composites such as thermal stability, hygroscopic properties, Brønsted-Lewis acidities, surface area and also crystallinity of the HZSM-5 support were obtained from these analyses. In the next step, we studied the possible uses of these composites as supported solid acid catalysts for Fischer indole reactions of phenyl hydrazine with variety of ketones and few aliphatic aldehydes at solvent-free medium at different temperatures.

FT-IR analysis

FTIR stretching and bending vibrations for the support HZSM-5 and hybrid samples of Zn²⁺ (**2a-2e**) primarily distinguished various structural constituents and crystallinity related to their characteristic occupancy in zeolite framework (**Fig.4B.1**, **Table 4B.1**).

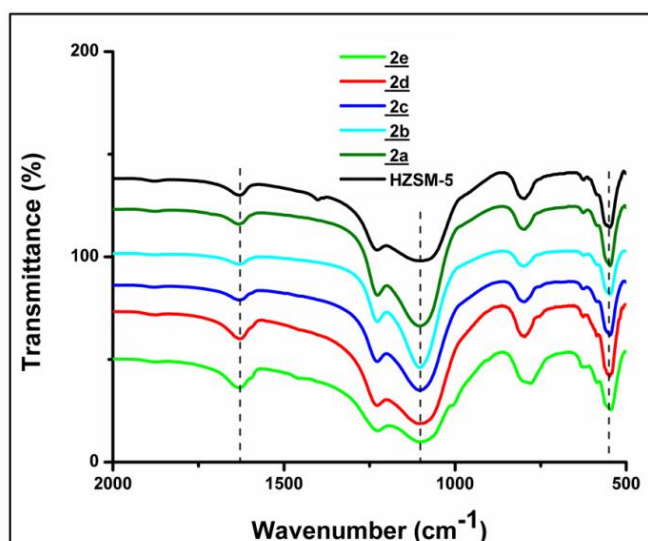


Fig.4B.1: FTIR spectra of **1**@HZSM-5 (**2a-2e**) & HZSM-5

Table 4B.1: FTIR peaks assignment of **1**@HZSM-5

Peaks (cm^{-1})	Assignment
450	T-O bending vibrations of the TiO_4 (T = Si or Al) internal tetrahedron
543-553	Double five ring lattice vibration of external linkages
797-801	External symmetric vibrations of T-O-T linkage (T = Si or Al)
1075	Asymmetric stretching vibration of $-\text{SO}_3\text{H}$ group is overlapped with asymmetric T-O band
1106-1230	Internal asymmetric stretching vibrations of T-O-T linkage
1630	Bending vibration due to adsorbed water on HZSM-5 framework merged with C=N stretching vibration of imidazolium cation

Evidence for existence of crystalline phases in all the modified materials of $[\text{Dsim}]_2[\text{ZnCl}_4]$ @HZSM-5 was determined as discussed for $[\text{Dsim}]_2[\text{NiCl}_4]$ /HZSM-5 in subunit **3B.1**. Estimation of degree of crystallinity from the ratio of intensities of the two peaks at 543 and 450 cm^{-1} [32, 33] gave the value in 0.78-0.82 range (**Table 4B.2**, **Fig.4B.2**) which was in accordance with the reported value 0.8 for pure HZSM-5 [34, 35]. Loss of some percent crystallinity in case of 50% loaded material was observed (**Table 4B.2**, optical density ratio > 0.85) (**2e**) which was later confirmed by PXRD analysis. Destruction of framework was justified from the IR pattern displaying additional peak at 1592 cm^{-1} as well as some discrepancy around 797-801 cm^{-1} .

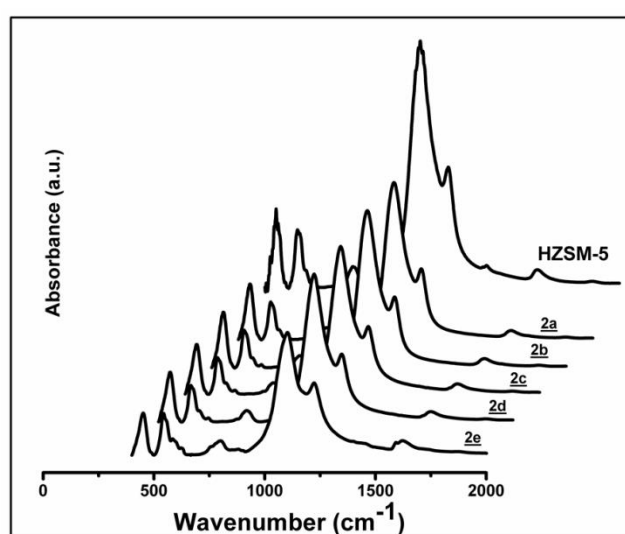
**Fig.4B.2:** IR absorbance spectra of **1**@HZSM-5 (**2a-2e**)

Table 4B.2: Optical density calculation from IR absorbance spectra

Entry	Optical density ratio					
	HZSM-5	<u>2a</u>	<u>2b</u>	<u>2c</u>	<u>2d</u>	<u>2e</u>
<u>1</u> @HZSM-5	0.83	0.80	0.78	0.81	0.82	0.99

Optical density ratio=Absorbance at 556 cm^{-1} /Absorbance at 450 cm^{-1}

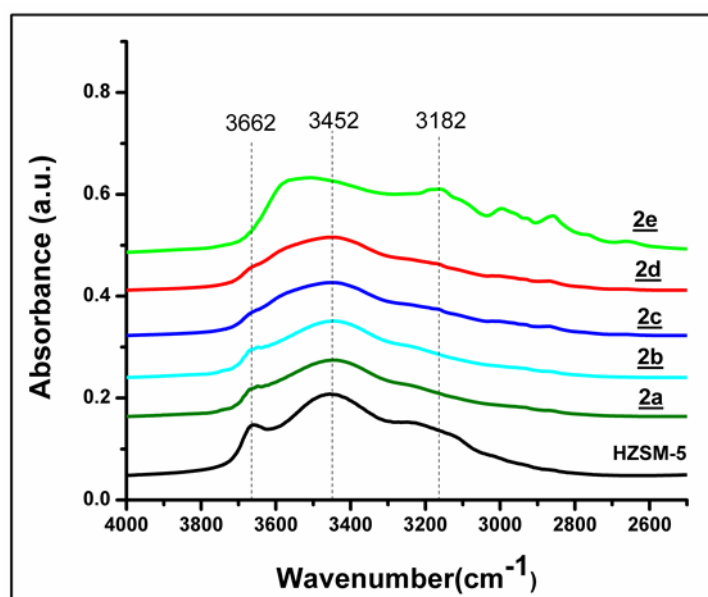
**Fig.4B.3:** OH stretching vibrations of 1@HZSM-5 (2a-2e)

Fig.4B.3 displayed the O-H stretching vibration of hybrid samples within frequency range 3000-3800 cm^{-1} . The behavior showed by highest loaded composite can be reasoned as framework discontinuity due to possible insertion and reinsertion of Al atoms associated with zeolite network. Reduction of peak intensity at 3662 cm^{-1} from 3% (2a) to 17% (2d) indicated the reinsertion of EFAl (extraframework Al) species into the zeolite as framework Al. Also, the shifting of absorption maximum of hydroxyl nests from 3452 cm^{-1} to 3610 cm^{-1} as broad band and occurrence of absorption peak between 2800-3200 cm^{-1} in 50% loaded hybrid sample can be reasoned as acid mediated insertion of Al and alkali mediated desilication of highly siliceous HZSM-5 structure respectively as described in the previous chapter (**Chapter 3**, subunit **3B.1**). Therefore, comparable thermal stabilities were obtained for the 50% loaded samples (2e) and the bare ionic salt (1) in TGA analysis (**Fig.4B.4**).

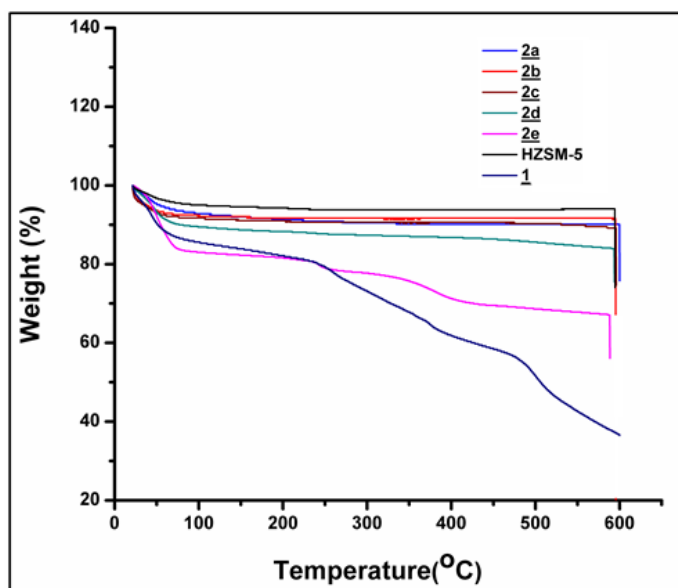
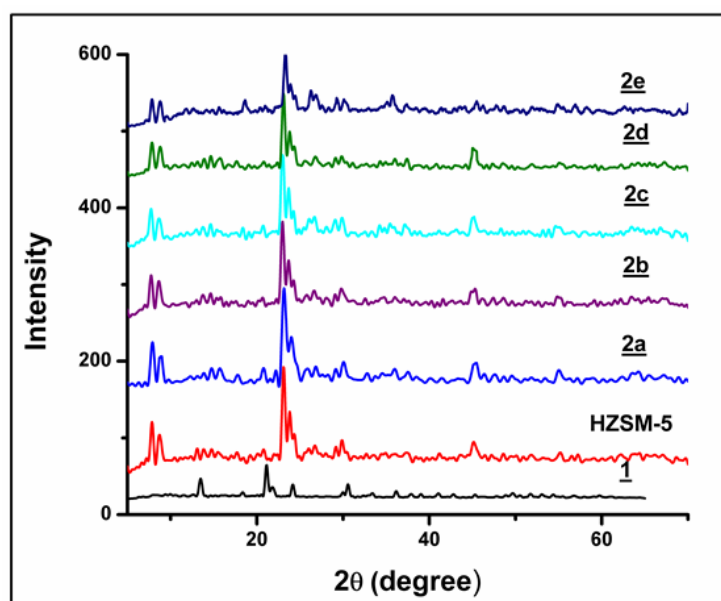
Thermogravimetric analysis

Fig.4B.4: TGA graph of 1@HZSM-5 (2a-2e), HZSM-5 & 1

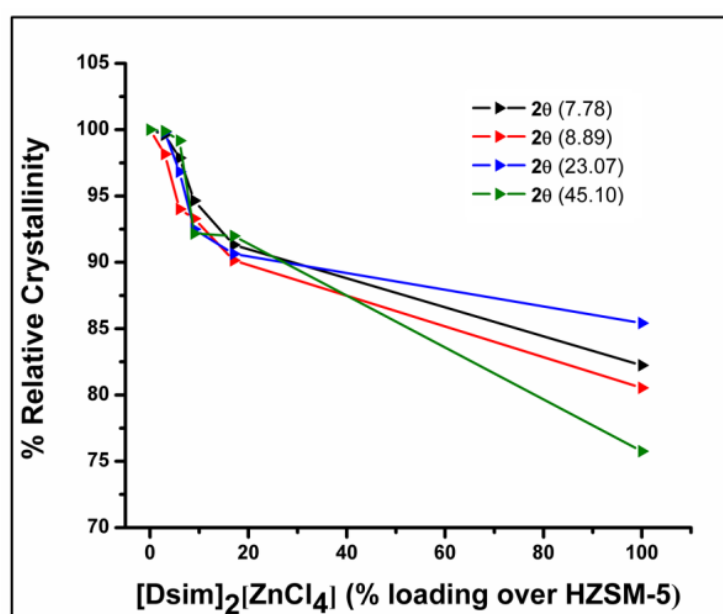
All the samples displayed 3-8% weight loss below 100°C in TGA profile (**Fig.4B.4**) which may be attributed to the loss of absorbed moisture. Above 100°C, 2a-2d (3-17%) expresses high thermal stability up to 600°C similar to that of parent HZSM-5. But the 50% loaded material 2e behaved like bare ionic salt due to presence of greater amount of hygroscopic salt in the composite.

Powder XRD analysis

Identical pattern of powder X-ray diffraction peaks in case of 1@HZSM-5 (2a-2d) and parent zeolite (**Fig.4B.5(a)**) strongly established the retention of crystallinity in synthesized materials 2a-2d without displaying any characteristic peak of the original ionic salt. However, decrease in peak intensity at $2\theta = 7.78, 23.07, 45.1$ was observed for the highest loaded material (50%, 2e) [36, 37]. The crystallinity values obtained from percent crystallinity graph of the loaded materials for the four intense peaks in the region $2\theta = 8-45^\circ$ with respect to the HZSM-5 (**Fig.4B.5(b)**) indicate gradual loss of crystallinity of 1@HZSM-5 materials up to the 17% loading (**Table 4B.3**). As observed from the **Fig.4B.2** and **Fig.4B.4**, the sample 2e has lost maximum crystallinity due to its hydrophilic nature and thus destabilization results from the dissolution of the HZSM-5 framework.



(a)

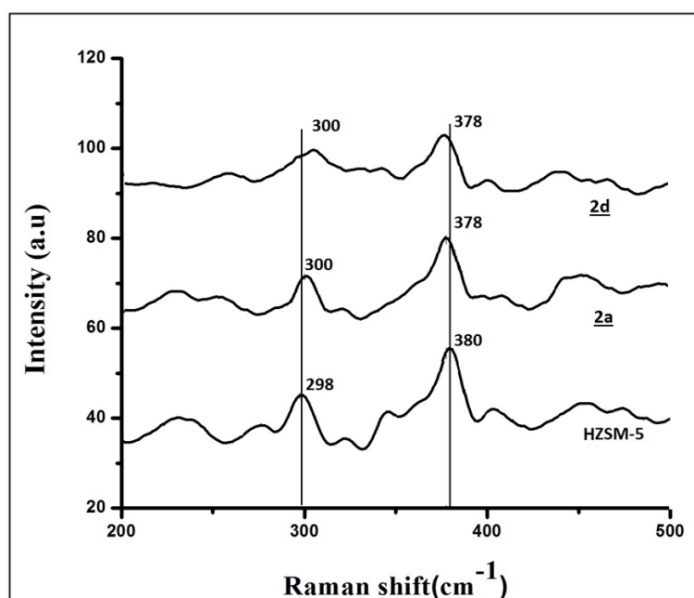


(b)

Fig.4B.5: (a) PXR D patterns of **1**@HZSM-5 (**2a-2e**), HZSM-5 & **1** and (b) Percentage crystallinity graph of **1**@HZSM-5 (**2a-2e**) with respect to parent HZSM-5

Table 4B.3: Relative % crystallinity table for the hybrid materials

2θ (degree)	Relative % crystallinity					
	HZSM-5	<u>2a</u>	<u>2b</u>	<u>2c</u>	<u>2d</u>	<u>2e</u>
7.78	100	99.61	97.88	94.65	91.32	82.23
8.89	100	98.16	94.02	93.30	90.15	80.54
23.07	100	99.82	96.83	92.50	90.64	85.42
45.10	100	99.89	99.17	92.17	91.99	75.76

Raman spectra**Fig.4B.6:** Raman spectra of 1@HZSM-5 (2a & 2d) with respect to parent HZSM-5

We chose to consider only materials of 1@HZSM-5 up to 17% loading (2d) because of the ambiguous behavior of the highest loaded hybrid 2e. Raman spectra for the lowest (3%) and highest loaded materials (17%) with respect to the parent HZSM-5 showed (**Fig.4B.6**) characteristic peaks which evidenced intactness of the MFI topology of HZSM-5 in the hybrid materials. The characteristic symmetric stretching modes of Si-O-Si bonds of five-membered silicate frameworks of MFI unit structure appeared at 290, 380, 460 cm^{-1} [38]. The basic peak of the HZSM-5 at 298 cm^{-1} is slightly shifted to 300

cm^{-1} and 295 cm^{-1} due to the presence of $\text{Zn}(+2)$ while the other important peak at 460 cm^{-1} changed its area to some extent.

SEM & EDX analysis

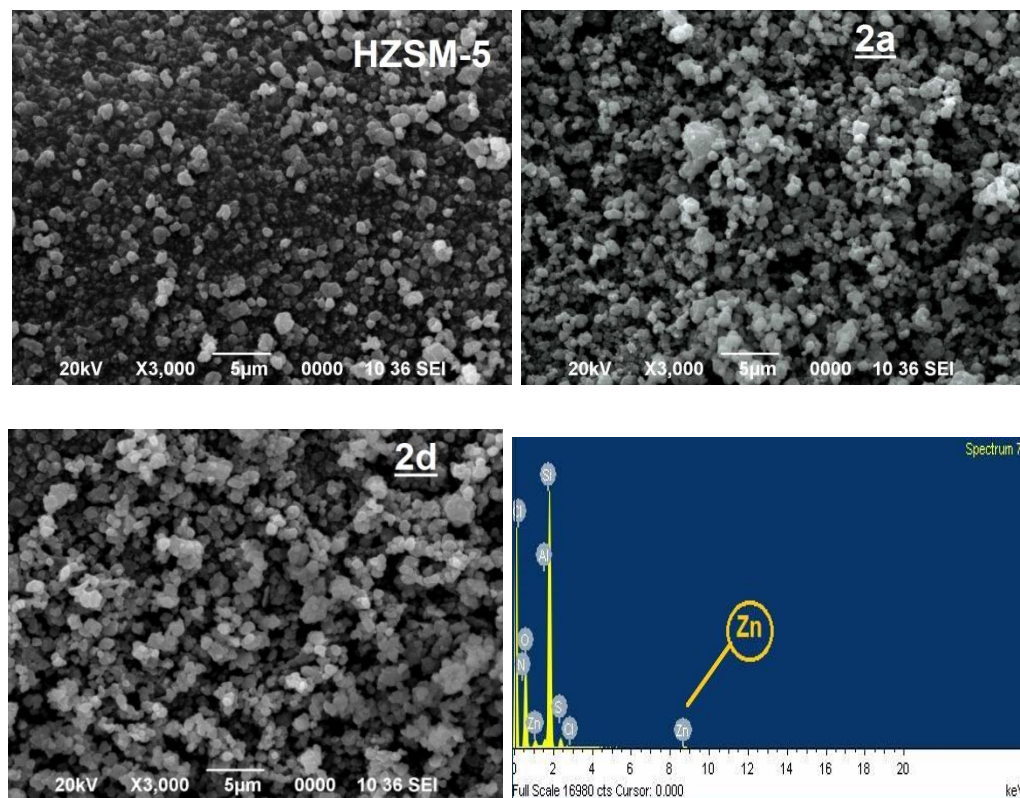


Fig.4B.7: SEM & EDX images of **2a**, **2d** and HZSM-5

SEM analyses of **2a** & **2d** along (Fig.4B.7) with HZSM-5 assessed the surface morphological changes and discrepancies resulted from loading of ionic salt **1** on HZSM-5. A little aggregation on the surface of lowest loaded composite **2a** with negligible change in crystalline phase was induced while **2d** showed clogging of pores with some cluster formation due to expected H-bonding occurred between Brønsted acidic sites of the ionic salt with framework Al generated from realumination of EFAl to the parent HZSM-5 as explained from Fig.4B.3. The EDX image of **2d** confirmed the presence of metal precursor $\text{Zn}(+2)$ along with Al, Si, Cl, N, O and S of the hybrid material **1**@HZSM-5.

Hammett acidity determination by UV-Visible

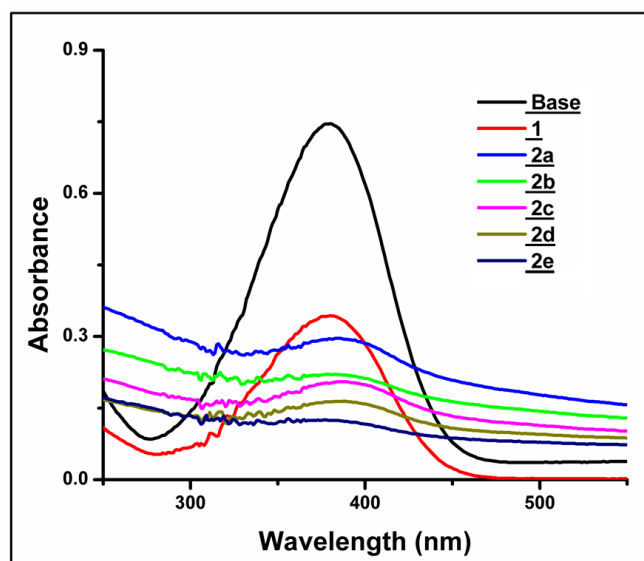


Fig.4B.8: Hammett plot of 1@HZSM-5 in ethanol

The trend in Brønsted acidity change in loaded zeolite material 1@HZSM-5 (2a-2d) was determined using Hammett plot on an UV-Visible spectrophotometer (**Fig.4B.8**) (referred to **Section 2B**). The acidity order of all these composite materials can be arranged with reference to the parent ionic salts as: 2d>2c>2b>2a>1 (**Table 4B.4**). The reason behind this increasing trend in Brønsted acidity towards the highest loaded sample can be predicted as increased acidic sites in composites already discussed in **Section 3B** (subunit **3B.1**).

Table 4B.4: Hammett acidity values of [Dsim]₂[ZnCl₄]1@HZSM-5

Entry	A_{\max}	[I]%	[IH ⁺]%	H ⁰
Base	0.745	100	0	-
<u>1</u>	0.343	46.06	53.96	0.92
<u>2a</u>	0.296	39.73	60.27	0.80
<u>2b</u>	0.221	29.66	70.34	0.61
<u>2c</u>	0.205	27.51	72.49	0.56
<u>2d</u>	0.166	22.28	77.72	0.44
<u>2e</u>	0.124	16.64	83.36	0.29

$A_{\max} = 380 \text{ nm}$

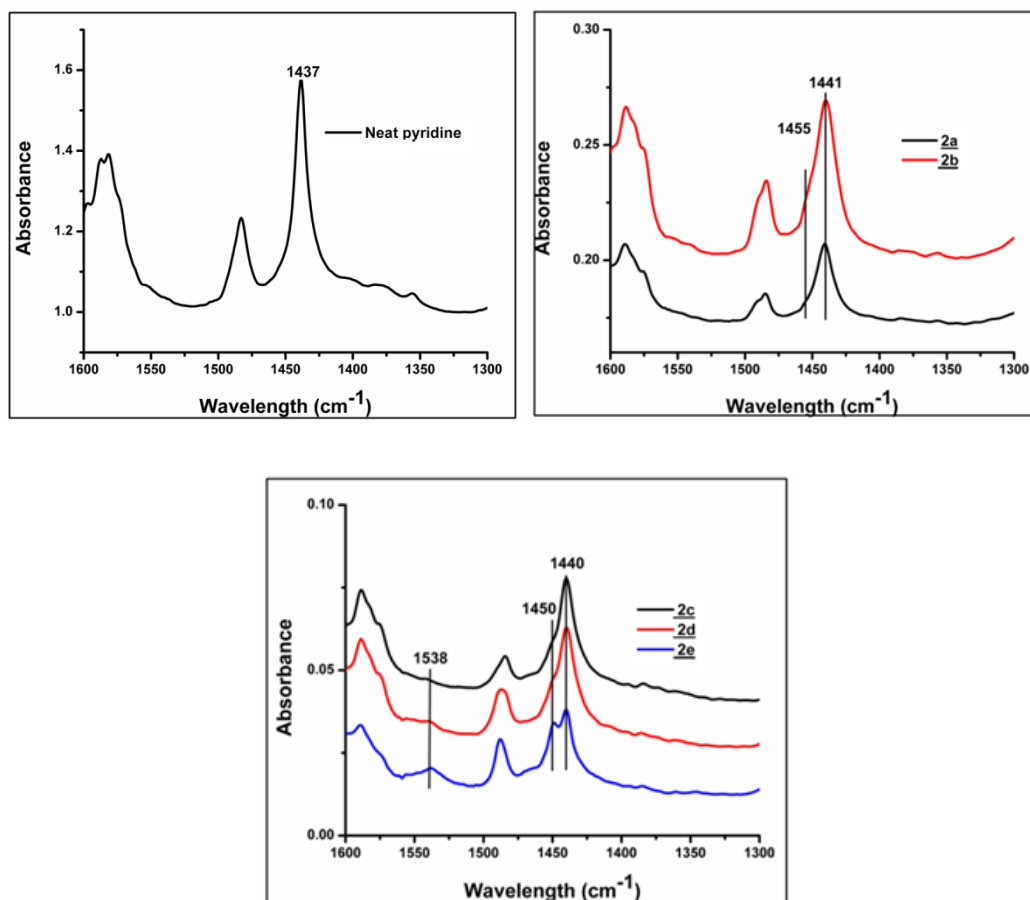
Lewis acidity determination

Fig.4B.9: FTIR analysis of Lewis acidity determination of **1**@HZSM-5 using pyridine

Lewis acidic sites of the synthesized materials (**2a-2e**) were determined using FTIR analysis which was done by mixing pyridine: **1**@HZSM-5 (1:3) for all the samples. As probe molecule neat pyridine displays characteristic bands at 1437 cm^{-1} which was shifted to higher value in case of Lewis acidic materials 1440 cm^{-1} along with shoulder broadening at $1450\text{-}1455\text{ cm}^{-1}$ (**Fig.4B.9**). This can be assumed as the Lewis acidity of materials contributed by ZnCl_4^{2-} anion in ionic salt. In the higher loaded materials **2c-2e**, a new absorbance peak at 1538 cm^{-1} appeared which may be explained as the interaction between chlorometallate with pyridine to form pyridinium ion. However, in **2a** and **2b** this peak was absent. This can be reasoned as the minimal percent loading of ionic salt on HZSM-5 which was not sufficient to express the formation of pyridinium ion in FTIR spectra [39]. From the Lewis acidity study it was found that the higher percent loaded samples exhibit more Lewis acidity.

UV/Vis diffuse reflectance spectra

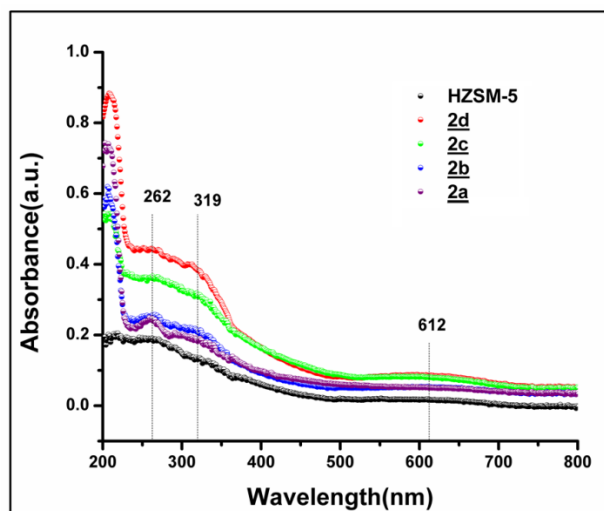


Fig.4B.10: UV-Visible DRS spectra of **1**@HZSM-5 (**2a-2d**) with respect to HZSM-5

To examine the effect of loading percentage of ionic salt UV/Vis diffuse reflectance spectra of loaded materials were recorded with respect to HZSM-5 (**Fig.4B.10**). All the absorptions clearly establish the existence of characteristic constituents of chlorometallate moiety in the immobilized materials. Intra ligand charge transfer transitions of the loaded ionic salt **1** at 222 nm and 340 nm can be correlated with the weak absorptions at 260 nm and 319 nm in the spectra of **1**@HZSM-5 (**2a-2d**) [3].

BET analysis

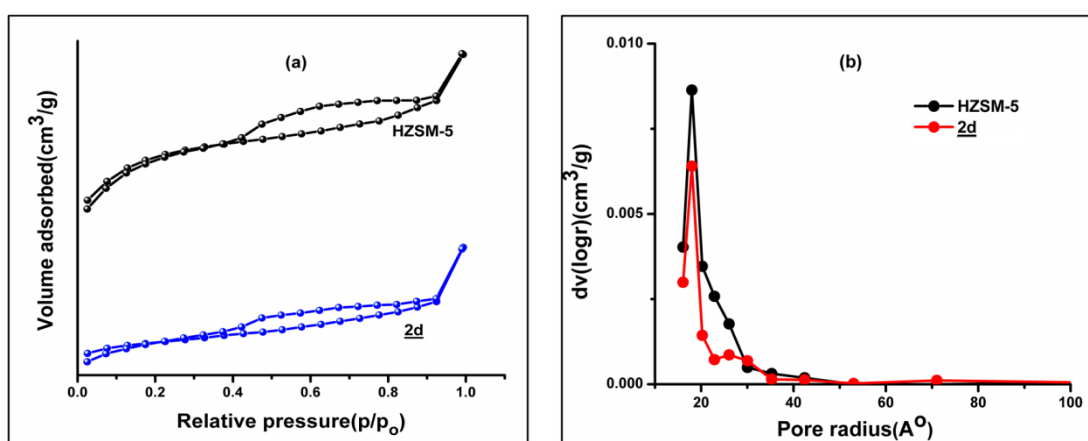


Fig.4B.11: (a) N_2 -isotherm of HZSM-5 and **2d** (b) BJH curve of HZSM-5 and **2d**

N_2 -isotherm of HZSM-5 and **2d** (**Fig.4B.11(a)**) displayed combined **type I** and **type IV** isotherm with type-H4 hysteresis loop which indicates the formation of a hierarchical

porous system containing both micropores and mesopores. Similar case of capillary condensation in $[\text{Dsim}]_2[\text{NiCl}_4]/\text{HZSM-5}$ from the previous chapter (**Chapter 3, Section 3B**) was also noticed in **1**@HZSM-5 in the region of $0.4 < P/P_0 < 0.95$ [40-42]. BJH pore size distribution plot for parent HZSM-5 with **2d** (17%) (**Fig.4B.11(b)**) was obtained using only adsorption branch of the isotherm from which the mean size of the micropores in both parent HZSM-5 and **2d** was estimated to be about 17.34 \AA (1.7 nm).

Fig 4B.12 represents the t-plots of HZSM-5 and **2d** obtained using the equation given by De Boer (details in **Chapter 3, Section 3B**). External surface areas and mesoporous areas were determined from the slopes of the straight lines derived from t-plots of respective samples ($A \text{ (m}^2 \text{ g}^{-1}) = \text{slope} * 15.47$) [43].

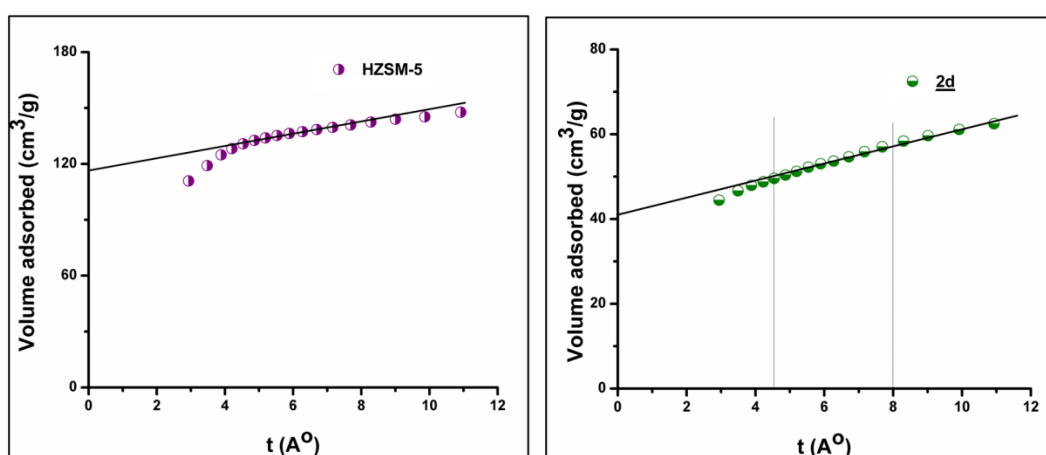


Fig.4B.12: t-plots of HZSM-5 and **2d**

Table 4B.5 summarized the results obtained from N_2 adsorption desorption isotherm, BJH curve and t-plots. The results expressed significant decrease in BET surface areas towards highest loaded material as compared to HZSM-5 which can be justified as clogging or filling of pores by loaded ionic salt

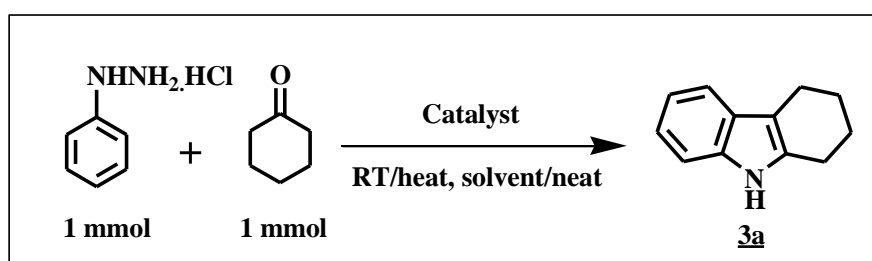
Table 4B.5: Summary of BET analysis

Entry	$S_{\text{BET}}^{\text{a}}$ (m^2/g)	$S_{\text{EXT}}^{\text{b}}$ (m^2/g)	V_{mp}^{b} (cm^3/g)	S_{mp}^{c} (m^2/g)
HZSM-5	428.77	53.34	0.178	375.43
2d	134.94	33.97	0.064	100.97

^a Surface area calculated form multipoint BET; ^b External surface areas and micropore volumes are measured by t-plot method; ^c $S_{\text{mp}} = S_{\text{BET}} - S_{\text{EXT}}$

4B.2 Catalytic performance

All the synthesized materials were utilized as catalysts in Fischer indole reaction to synthesize indole derivatives using phenyl hydrazine hydrochloride and various ketones and aldehydes. Catalytic study of these materials included optimization of the catalyst amount, reaction temperature, different solvent and synthesis of library of indole derivatives using optimized condition. **Scheme 4B.1** was taken as model reaction to optimize the reaction condition which involved phenylhydrazine hydrochloride (1 mmol) and cyclohexanone (1 mmol) to yield 1, 2, 3, 4-tetrahydrocarbazole (**3a**) in presence of varied (5, 10 and 15 mg) amount of (**2a-2d**) catalyst in solvent-free medium at 100°C (**Table 4B.6**, entry 1-4). 10 mg of the 17 % loaded ionic salt **2d** (**Table 4B.6**, entry 4) was considered as the most efficient catalyst at 100°C as well as optimized temperature of 80°C (**Table 4B.6**, entry 5). Three solvents CH₂Cl₂, EtOH and H₂O were used to study the solvent effects at temperatures below their boiling points and they showed good results (**Table 4B.6**, entry 6). **Table 4B.7** mentioned some reported data for comparison of the percentage yields of model product **3a** for the present catalyst and previously reported ones [44, 22, 25-27]. Substrate scope study was done with different cyclic, acyclic or aromatic keto and aliphatic aldehyde compounds with 10 mg of the **2d** catalyst at 80-90°C to synthesize substituted indole derivatives (**Table 4B.8**). Excellent results were achieved for the keto compounds corresponding to product yield, easy isolation and minimal side product but in case of two aliphatic aldehydes we used i.e. propionaldehyde and isobutyraldehyde these results were unlikely. The reaction involving two aliphatic aldehydes was accompanied by a complex mixture of side products which were difficult to remove and we could not isolate the pure product. Therefore, these two aldehydes were discarded from **Table 4B.8**.



Scheme 4B.1: Synthesis of 1, 2, 3, 4-tetrahydrocarbazole

Table 4B.6: Optimization of the catalyst amount for the synthesis of **3a**

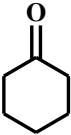
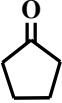
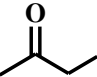
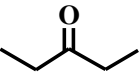
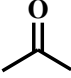
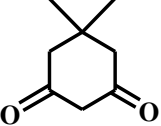
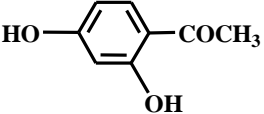
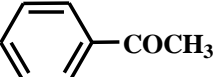
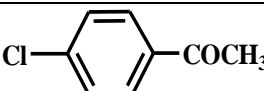
Entry	Catalyst	Time (h)			% Yield ^{a, b}		
		5 mg	10 mg	15 mg			
1	1 @HZSM-5=3% (2a)	2.75	2.5	1.75	75	80	82
2	1 @HZSM-5=6% (2b)	2.75	2.5	1.75	80	82	82
3	1 @HZSM-5=9% (2c)	2	1.5	1.5	85	88	88
4	1 @HZSM-5=17% (2d)	1.5	0.75	0.5	88	95	95
5	-do- ^c	24/1/ 0.75 /0.75 ^c			-/75/ 94 /95 ^c		
6	-do- ^d	0.83/1/1.16			90/82/90 ^d		

^a Isolated yield; ^b Reactions of entries 1-4 were conducted at 100°C in neat condition; ^c Reactions were conducted at room temperature, 60°C, 80°C and 100°C respectively using 10 mg of the **2d** in neat condition; ^d Reactions were performed in CH₂Cl₂, EtOH and H₂O respectively at temperatures below their boiling points using 10 mg of **2d** as catalyst.

Table 4B.7: Comparison of catalytic activity of **2d** with different catalysts

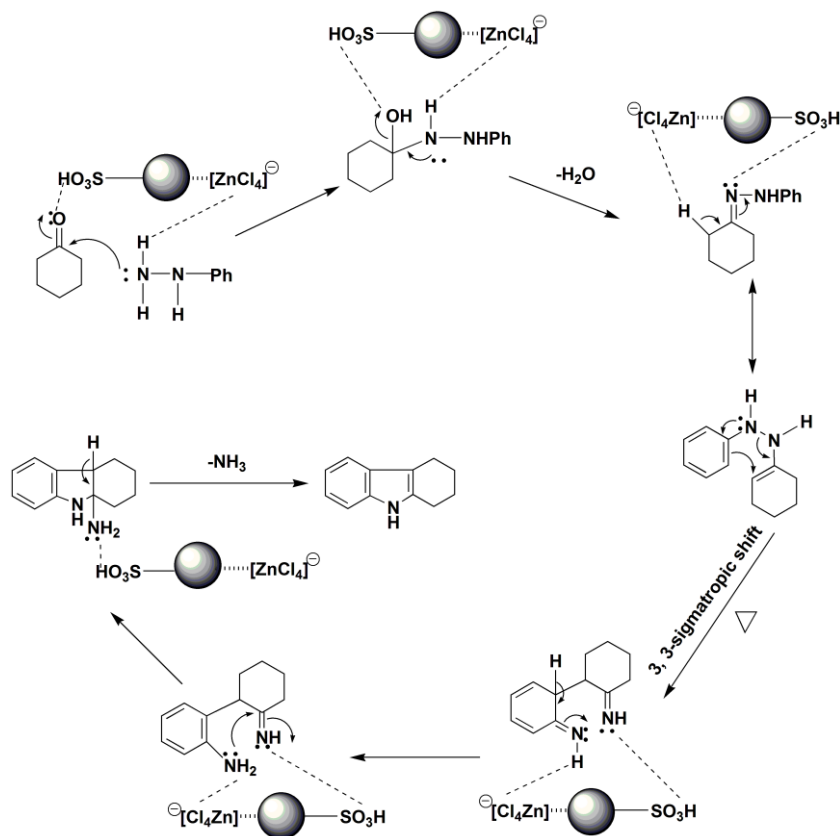
Catalysts	Reaction condition	Time (h)	% Yield (3a)
1 @HZSM-5 = 17% (2d)	10 mg, 100°C	0.75	94
1 [Dsim] ₂ [ZnCl ₄]	-do-	1.5	75
<i>p</i> -toluene sulfonic acid	-do-	8	68
ZnCl ₂	-do-	6	70
H-Y	1g, MeOH, 60°C	18	69.3 [44]
[bmim][HSO ₄]	70°C in IL	1	92 [22]
50 mol% [cmmim][BF ₄]	140°C	2	92 [25]
20 mol % [bmim][BF ₄]	Reflux in MeOH	7	95 [26]
10 mol % [C ₁₀ MIM][Br]	MW, 300 W	3 min	58.05 [27]
10 mol % of [C ₁₀ MIM][Br]+ZnCl ₂	MW, 300 W	-do-	94.25 [27]

Table 4B.8: Substrate scope study of indole derivatives using **1**@HZSM-5 = 17% (**2d**) as catalyst

Entry	Ketone	Time (h)	Product	% Yield of product ^a
1		0.75	3a	94
2		1	3b	90
3		0.83	3c	90
4		0.83	3d	90
5		0.75	3e	92
6		1	3f	82
7		1	3g	80
8		0.75	3h	88
9		0.75	3i	85

^aIsolated yield***Plausible reaction mechanism***

The plausible reaction mechanism can be understood as simultaneous interactions of both the Brönsted-Lewis acidic sites of the supported catalyst with C=O and also with -NHNH₂ groups through H-bonding as portrayed in **Scheme 4B.2**.



Scheme 4B.2: Mechanism of Fischer indole synthesis catalyzed by **1**@HZSM-5 = 17% (**2d**)

Recyclability study

To investigate the recyclability of the spent catalyst the model reaction (**Scheme 4B.1**) was carried out for 5 mmol scale of the substrates using 50 mg of **2d** as solid acidic catalyst under standard reaction condition. After completion of the reaction monitored by TLC, dichloromethane was used to dissolve the reaction mixture where the catalyst was insoluble and thus separated out from the organic extract upon decantation. In the next step, the spent catalyst was reactivated by washing 2-3 times with absolute ethanol and then dried in vacuum oven at 100°C for 1 h. The oven dried catalyst was reused for nine more cycles following the same recyclability procedure (**Fig.4B.13**). Reused catalyst was subjected to ICP-OES and PXRD analysis (**Table 4B.9** & **Fig.4B.14**). ICP-OES data (**Table 4B.9**) indicated the slight leaching of metal content in every alternate cycle which may be accounted for *in situ* formation of base from the ionic salts and thus causes desilication of HZSM-5 support after repeated ethanol washing and drying at 100°C during work-up procedure. This limits the reactivation of the used catalyst containing excess ionic salt.

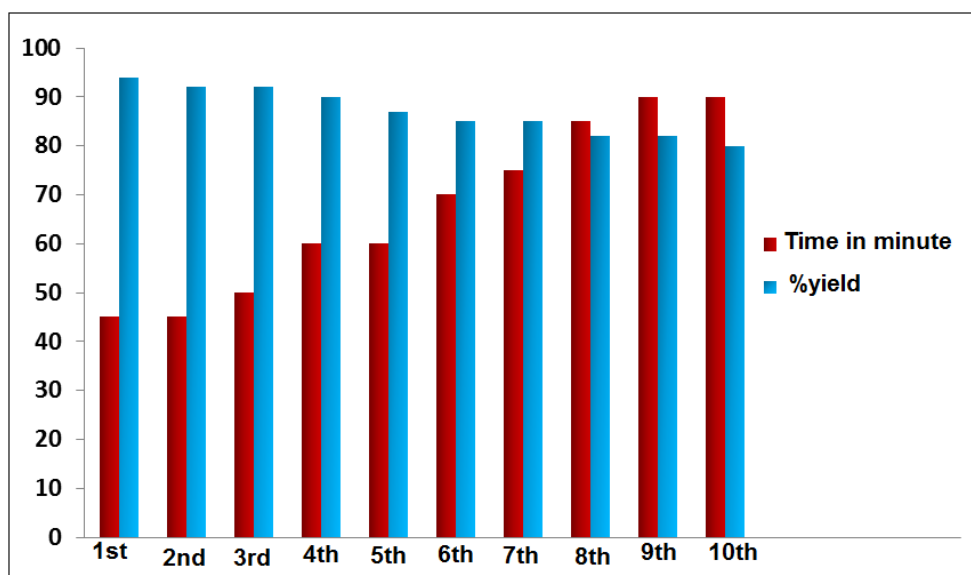


Fig.4B.13: Recyclability profile of **2d**

Table 4B.9: ICP-OES results of recycled **2d**

Entry	Cycle	Amount of Zn (mg/L)
1	2 nd	7.43
2	4 th	6.95
3	6 th	6.38
4	8 th	5.27
5	10 th	4.91

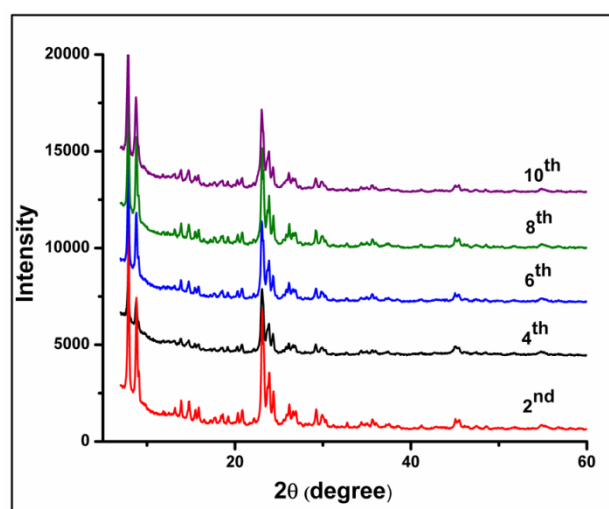


Fig.4B.14: PXRD pattern of recycled **2d** alternative cycles

4B.3 Conclusion

This work competently described the synthesis and characterization of 1, 3-disulfoimidazolium chlorozincate@HZSM-5 hybrid materials and their catalytic efficiency as dual acidic catalyst in Fischer indole reaction of phenylhydrazine hydrochloride with aliphatic/aromatic ketones. Significant surface area and excellent thermal stability of these heterogeneous materials proved them as potent candidate for acid catalyzed synthesis of indole derivatives. ZnCl_4^{2-} played key role in this catalytic process by imparting Lewis acidity which enhanced the efficiency together with the Brønsted acidity of the catalyst. A great advantage of limiting the hygroscopic nature of the ionic salt came from HZSM-5 as support and thus upgrading their stability as excellent heterogeneous catalyst. All these facts and above discussion made a conclusion that the dual acidic hybrid materials can be considered as better alternative for acid catalysis in organic synthesis in comparison to conventional acids and other acidic catalysts. Fascinating abilities of these catalysts lies in the possession of all the properties by HZSM-5 similar to heterogeneous catalysts in conjunction with the dual acidic character contributed by Lewis acid ZnCl_4^{2-} and Brønsted acid group $-\text{SO}_3\text{H}$. These bring selectivity to the product without formation of many unwanted side products followed by simple isolation and easy recyclability leading catalysis towards its best. This work opens an easy and beneficial route in the field of heterogeneous catalysis.

4B.4 Experimental section

General techniques

All the techniques used in this section are similar to that of previous section (**Section 3B**, subunit **3B.4**). ^1H and ^{13}C NMR spectra for all the synthesized compounds were recorded on JEOL 400 MHz spectrophotometer (δ in ppm) in CDCl_3 . CHN analysis was carried out using Perkin Elmer CHN analyzer (2400 series 2).

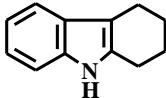
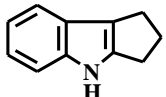
Preparation of $[\text{Dsim}]_2[\text{ZnCl}_4]@\text{HZSM-5}$

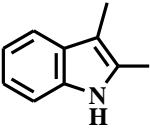
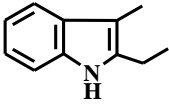
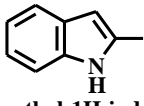
Preparation method of the five composites of $[\text{Dsim}]_2[\text{ZnCl}_4]@\text{HZSM-5}$ was done according to the procedure described in **Section 3B** (subunit **3B.4**) for the preparation of $[\text{Dsim}]_2[\text{NiCl}_4]/\text{HZSM-5}$ composites.

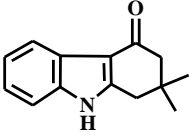
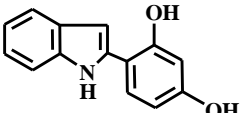
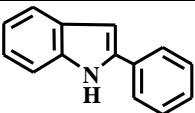
Fischer indole reaction

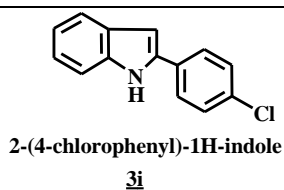
A typical reaction of phenylhydrazine hydrochloride (1 mmol) with various aliphatic or aromatic ketones and aliphatic aldehydes (1 mmol) using catalytic amount (10 mg) of $[\text{Dsim}]_2[\text{ZnCl}_4]@\text{HZSM-5}$ was performed at 80-100°C in neat condition for the specific reaction time to afford the respective indole derivatives. The product formation was monitored by thin layer chromatography using 1:5 EtOAc: hexane as mobile phase. After that the reaction mixture was cooled immediately to room temperature and extracted the organic mixture with dichloromethane (DCM). The catalyst was insoluble in DCM. Thus decantation of DCM with further washing for several times using the same solvent gave the recycled catalyst. Then the organic phase was dried over Na_2SO_4 and the solvent was removed in a rotary evaporator. Recrystallization from ethanol and water gave us the desired solid product in satisfactory yield. This process was repeated for 2-3 times to obtain analytically pure product.

4B.5 Spectral data of indole derivatives (3a-3i)

Entry	Spectral data
 <p>6,7,8,9-tetrahydro-5H-carbazole 3a</p>	Off-white amorphous solid, Mp.: 112°C; FT-IR (KBr) cm^{-1} : 3397, 3049, 2923, 2843, 1625, 1440, 1365, 1239; ^1H NMR (CDCl_3 , 400 MHz): δ 1.83-1.94 (m, 4H), 2.68-2.74 (m, 4H), 7.03-7.12 (m, 2H), 7.28 (d, $J = 7.8$ Hz, 1H), 7.44 (d, $J = 7.3$ Hz, 1H), 7.67 (brs, 1H); ^{13}C NMR (CDCl_3 , 100 MHz): δ 20.9, 23.2, 23.3, 23.4, 110.4, 117.5, 119.2, 120.9, 127.4, 133.9, 135.7; CHN analysis $\text{C}_{12}\text{H}_{13}\text{N}$: Calcd. C, 84.17; H, 7.65; N, 8.18; Found: C, 84.12; H, 7.54; N, 8.16.
 <p>1,2,3,4-tetrahydrocyclopenta[b]indole 3b</p>	Maroon solid, Mp.: 96-98°C; FT-IR (KBr) cm^{-1} : 3400, 3043, 2920, 2833, 1620, 1430, 1362, 1235; ^1H NMR (CDCl_3 , 400 MHz): δ 2.03 (m, 2H), 2.49-2.54 (m, 2H), 2.79-2.87 (m, 2H), 7.06-7.07 (m, 2H), 7.27-7.30 (m, 1H), 7.41-7.43 (m, 1H), 7.82 (brs, 1H); ^{13}C NMR (CDCl_3 , 100

	MHz): δ 23.3, 25.2, 34.6, 110.6, 114.5, 119.0, 120.7, 122.6, 129.0, 131.3, 132.0; CHN analysis $C_{11}H_{11}N$: Calcd. C, 84.04; H, 7.05; N, 8.91; Found: C, 84.02; H, 7.00; N, 8.89.
 2,3-dimethyl-1H-indole 3c	Brown amorphous solid, Mp.: 102-104°C; FT-IR (KBr) cm^{-1} : 3400, 3050, 2909, 2849, 1624, 1463, 1392, 1242; 1H NMR ($CDCl_3$, 400 MHz): δ 2.22 (s, 3H), 2.35 (s, 3H), 7.04-7.12 (m, 2H), 7.25 (d, $J = 5.5$ Hz, 1H), 7.45 (d, $J = 6.4$ Hz, 1H), 7.66 (brs, 1H); ^{13}C NMR ($CDCl_3$, 100 MHz): δ 8.2, 11.5, 107.3, 110.2, 117.6, 118.9, 120.6, 129.2, 130.6, 134.8.; CHN analysis for $C_{10}H_{11}N$: Calcd. C, 82.72; H, 7.64; N, 9.65; Found: C, 82.70; H, 7.65; N, 9.62.
 2-ethyl-3-methyl-1H-indole 3d	White solid, Mp.: 43-44°C; FT-IR (KBr) cm^{-1} : 3362, 3029, 2957, 2924, 2860, 1610, 1551, 1485, 1360, 1239; 1H NMR ($CDCl_3$, 400 MHz): δ 1.27 (t, $J = 7.6$ Hz, 3H), 2.23 (s, 3H), 2.75 (q, $J = 7.6$ Hz, 2H), 7.06-7.13 (m, 2H), 7.27 (d, $J = 7.3$ Hz, 1H), 7.48 (d, $J = 7.8$ Hz, 1H), 7.71 (s, 1H); ^{13}C NMR ($CDCl_3$, 100 MHz): δ 8.3, 14.0, 19.5, 106.1, 110.0, 118.0, 118.8, 120.9, 129.5, 135.1, 136.4; CHN analysis for $C_{11}H_{13}N$: Calcd. C, 82.97; H, 8.23; N, 8.80; Found: C, 82.56; H, 8.18; N, 8.82.
 2-methyl-1H-indole 3e	White solid, Mp.: 57-59°C; FT-IR (KBr) cm^{-1} : 3436, 2925, 2853, 1600, 1494, 1249; 1H NMR ($CDCl_3$, 400MHz): δ 2.15 (s, 3H), 6.82 (t, $J = 7.3$ Hz, 1H), 7.02-7.04 (m, 2H), 7.20-7.24 (m, 2H); ^{13}C NMR ($CDCl_3$, 100 MHz): δ 16.1, 100.1, 112.8, 119.7, 128.3, 128.9, 145.4; CHN analysis for C_9H_9N : Calcd. C, 82.41; H, 6.92; N, 10.68; Found: C, 82.50; H, 6.95; N, 10.61.

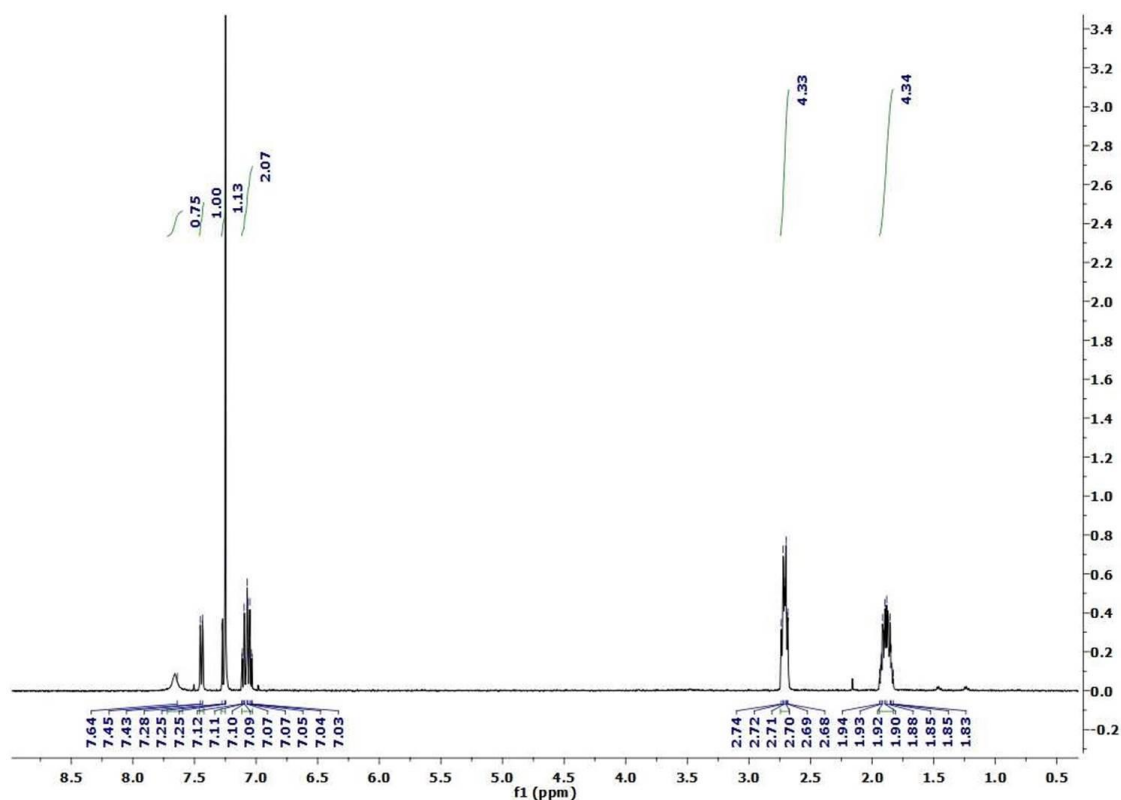
 <p>2,3-dihydro-2,2-dimethyl-1H-carbazol-4(9H)-one 3f</p>	<p>Reddish brown solid, Mp.: 190-194°C; FT-IR (KBr) cm^{-1}: 3422, 2959, 2865, 1607-1456, 1232 cm^{-1}; ^1H NMR (CDCl_3, 400 MHz): δ 1.05-1.10 (m, 6H), 2.20-2.28 (m, 4H), 7.20-7.32 (m, 4H); ^{13}C NMR (CDCl_3, 100 MHz): δ 28.0, 28.3, 33.1, 50.7, 52.8, 95.2, 97.8, 112.4, 120.7, 129.3, 197.3; CHN analysis for $\text{C}_{14}\text{H}_{15}\text{NO}$: Calcd. C, 78.84; H, 7.09; N, 6.57; Found: C, 78.72; H, 7.01; N, 6.60.</p>
 <p>4-(1H-indol-2-yl)benzene-1,3-diol 3g</p>	<p>Off-white amorphous solid, Mp.: 114-115°C; FT-IR (KBr) cm^{-1}: 3422, 2919, 2840, 1598, 1441, 1251; ^1H NMR (CDCl_3, 400 MHz): δ 6.38 (dd, $J = 2.7, 8.7\text{Hz}$, 1H), 6.45 (d, $J = 2.5\text{Hz}$, 1H), 6.92 (t, $J = 7.3\text{Hz}$, 1H), 7.00 (d, $J = 7.8\text{Hz}$, 2H), 7.09 (s, 1H), 7.27-7.31 (m, 3H); ^{13}C NMR (CDCl_3, 100 MHz): δ 103.8, 106.5, 113.03, 113.8, 120.2, 128.0, 129.5, 144.2, 148.3, 157.4, 159.9; CHN analysis for $\text{C}_{14}\text{H}_{11}\text{NO}_2$: Calcd. C, 74.65; H, 4.92; N, 6.22; Found: C, 74.55; H, 4.95; N, 6.20.</p>
 <p>2-phenyl-1H-indole 3h</p>	<p>Off-white amorphous solid, Mp.: 186-187°C; FT-IR (KBr) cm^{-1}: 3400, 2920, 2833, 1615, 1445, 1360, 1236; ^1H NMR (CDCl_3, 400 MHz): δ 6.90 (t, $J = 7.2\text{Hz}$, 1H), 7.20-7.28 (m, 2H), 7.30-7.34 (m, 3H), 7.38-7.49 (m, 4H), 7.98 (brs, 1H); ^{13}C NMR (CDCl_3, 100 MHz): δ 113.2, 120.1, 122.9, 125.6, 127.8, 128.3, 129.2, 133.2, 139.1, 141.1, 141.3, 145.1; CHN analysis for $\text{C}_{14}\text{H}_{11}\text{N}$: Calcd. C, 87.01; H, 5.74; N, 7.25; Found: C, 86.95; H, 5.72; N, 7.26.</p>

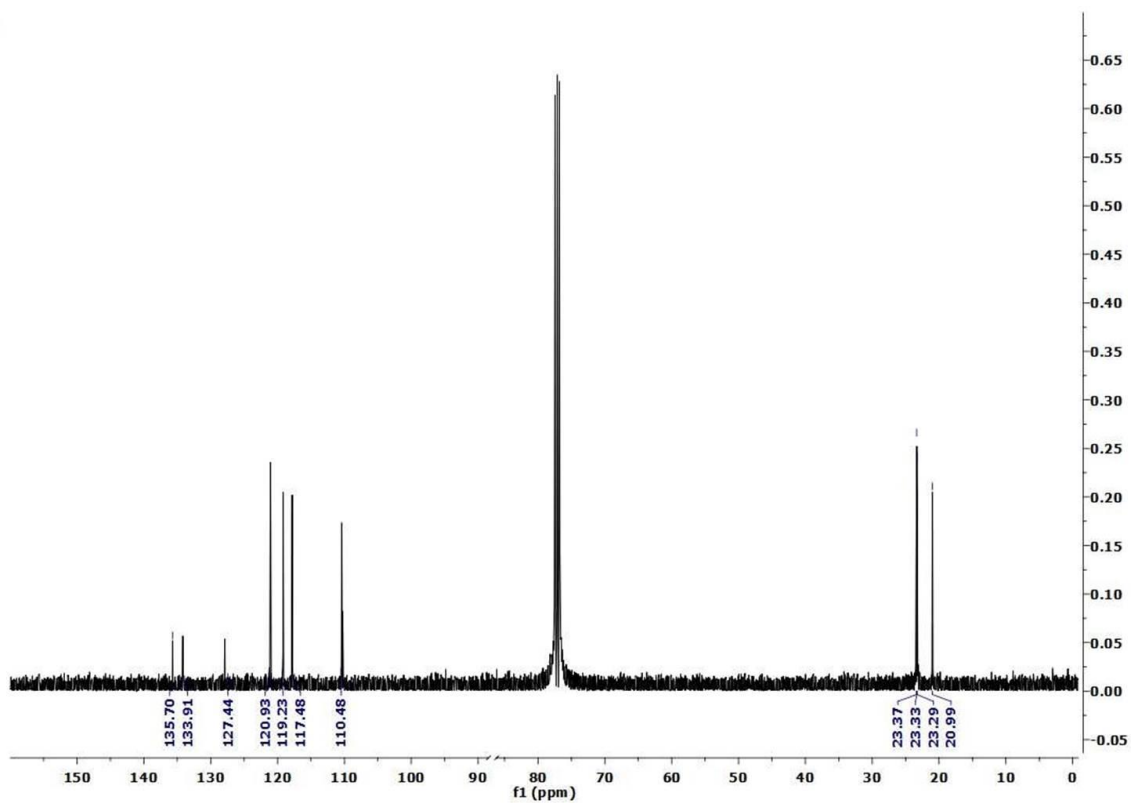
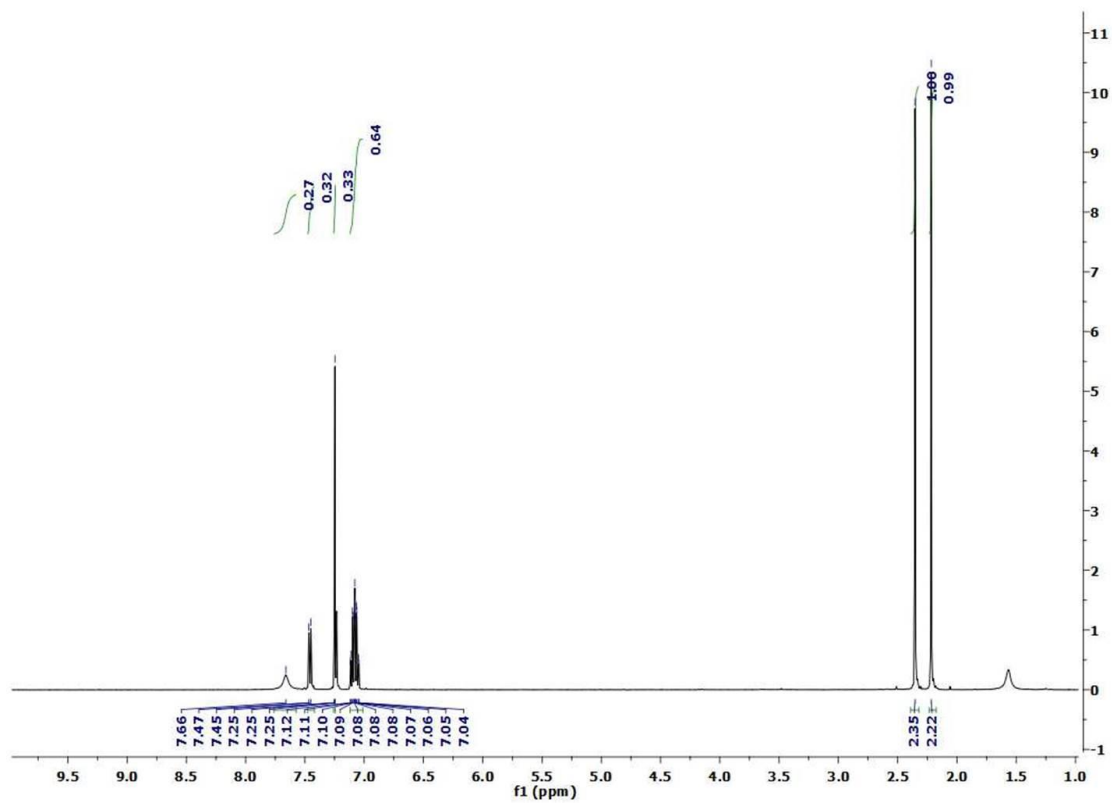


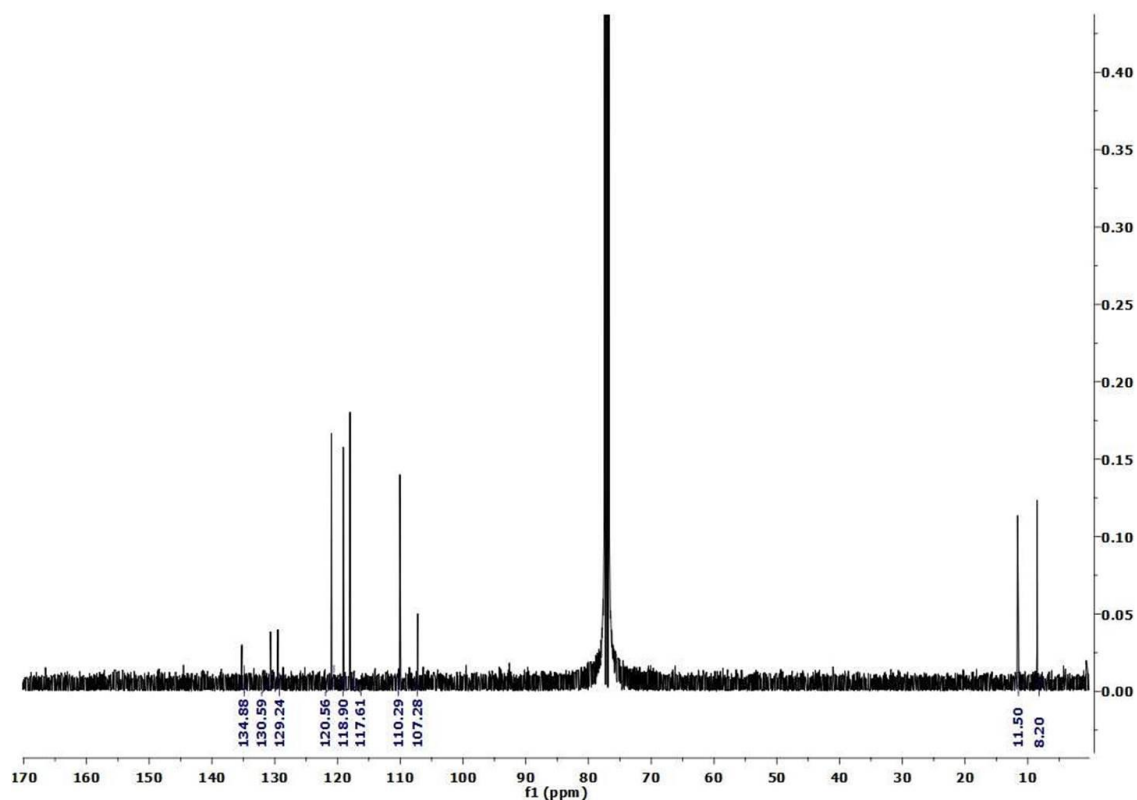
Off-white amorphous solid, Mp.: 193-194°C; FT-IR (KBr) cm^{-1} : 3394, 3045, 2920, 2841, 1615, 1438, 1362, 1235; ^1H NMR (CDCl_3 , 400 MHz): δ 6.86 (t, $J = 7.3$ Hz, 1H), 7.14-7.42 (m, 8H), 7.88 (brs, 1H); ^{13}C NMR (CDCl_3 , 100 MHz): δ 113.2, 120.5, 126.7, 128.5, 128.9, 129.3, 129.8, 135.3, 139.6; CHN analysis for $\text{C}_{14}\text{H}_{10}\text{ClN}$: Calcd. C, 73.85; H, 4.43; N, 6.15; Found: C, 73.56; H, 4.40; N, 6.15.

4B.6 NMR spectra of some selected compounds

1. ^1H NMR of **3a**



^{13}C NMR of **3a**2. ^1H NMR of **3c**

^{13}C NMR of **3c****References**

1. Fan, Y., Bao, X., Lin, X., Shi, G. and Liu, H. Acidity adjustment of HZSM-5 zeolites by dealumination and realumination with steaming and citric acid treatments. *The Journal of Physical Chemistry B*, 110(31):15411-15416, 2006.
2. Mehnert, C. P. Supported ionic liquid catalysis. *Chemistry-A European Journal*, 11(1):50-56, 2005.
3. Saikia, S., Gogoi, P., Dutta, A. K., Sarma, P. and Borah, R. Design of multifaceted acidic 1, 3-disulfoimidazolium chlorometallate ionic systems as heterogeneous catalysts for the preparation of β -amino carbonyl compounds. *Journal of Molecular Catalysis A: Chemical*, 416:63-72, 2016.
4. Gogoi, P., Dutta, A. K., Saikia, S. and Borah, R. Heterogenized hybrid catalyst of 1-sulfonic acid-3-methyl imidazolium ferric chloride over NaY zeolite for one-pot synthesis of 2-amino-4-arylpyrimidine derivatives: A viable approach. *Applied Catalysis A: General*, 523:321-331, 2016.
5. Kaushik, N., Kaushik, N., Attri, P., Kumar, N., Kim, C., Verma, A. and Choi, E. Biomedical importance of indoles. *Molecules*, 18(6):6620-6662, 2013.

6. Taber, D. F. and Tirunahari, P. K. Indole synthesis: a review and proposed classification. *Tetrahedron*, 67(38):7195-7210, 2011.
7. Robinson, B. The Fischer indole synthesis. *Chemical Reviews*, 63(4):373-401, 1963.
8. Miyata, O., Kimura, Y., Muroya, K., Hiramatsu, H. and Naito, T. Thermal cyclization of N-trifluoroacetyl enehydrazines under mild conditions: A novel entry into the Fischer indole synthesis. *Tetrahedron Letters*, 40(18):3601-3604, 1999.
9. Kissman, H. M., Farnsworth, D. W. and Witkop, B. Fischer indole syntheses with polyphosphoric acid. *Journal of the American Chemical Society*, 74(15):3948-3949, 1952.
10. Hegde, V., Madhukar, P., Madura, J. D. and Thummel, R. P. Fischer route to pyrido [3, 2-g] indoles. A novel receptor for urea derivatives. *Journal of the American Chemical Society*, 112(11):4549-4550, 1990.
11. Hillier, M. C., Marcoux, J. F., Zhao, D., Grabowski, E. J., McKeown, A. E. and Tillyer, R. D. Stereoselective formation of carbon-carbon bonds via S_N2 -displacement: Synthesis of substituted cycloalkyl [b] indoles. *The Journal of Organic Chemistry*, 70(21):8385-8394, 2005.
12. Nakazaki, M. and Yamamoto, K. Direct synthesis of indole by the Fischer indole synthesis. *The Journal of Organic Chemistry*, 41(10):1877-1877, 1976.
13. Ackermann, L. and Born, R. $TiCl_4/t-BuNH_2$ as the sole catalyst for a hydroamination-based Fischer indole synthesis. *Tetrahedron Letters*, 45(52):9541-9544, 2004.
14. Baccolini, G. and Todesco, P. E. Synthesis of 2, 3-disubstituted indoles under mild conditions. *Journal of the Chemical Society, Chemical Communications*, 11:563a-563a, 1981.
15. Mhaske, S. B. and Argade, N. P. Facile zeolite induced Fischer-indole synthesis: A new approach to bioactive natural product rutaecarpine. *Tetrahedron*, 60(15):3417-3420, 2004.
16. Lipińska, T., Guibé-jampel, E., Petit, A. and Loupy, A. 2-(2-Pyridyl) indole derivatives preparation via Fischer reaction on montmorillnite K10/zinc chloride under microwave irradiation. *Synthetic Communications*, 29(8):1349-1354, 1999.

17. Dhakshinamoorthy, A. and Pitchumani, K. Facile clay-induced Fischer indole synthesis: A new approach to synthesis of 1, 2, 3, 4-tetrahydrocarbazole and indoles. *Applied Catalysis A: General*, 292:305-311, 2005.
18. An, J., Bagnell, L., Cablewski, T., Strauss, C. R. and Trainor, R. W. Applications of high-temperature aqueous media for synthetic organic reactions. *The Journal of Organic Chemistry*, 62(8):2505-2511, 1997.
19. Fitzpatrick, J. and Hiser, R. Noncatalytic Fischer indole synthesis. *The Journal of Organic Chemistry*, 22(12):1703-1704, 1957.
20. Rebeiro, G. L. and Khadilkar, B. M. Chloroaluminate ionic liquid for Fischer indole synthesis. *Synthesis*, 2001(03):0370-0372, 2001.
21. Morales, R. C., Tambyrajah, V., Jenkins, P. R., Davies, D. L. and Abbott, A. P. The regiospecific Fischer indole reaction in choline chloride 2ZnCl_2 with product isolation by direct sublimation from the ionic liquid. *Chemical Communications*, 2:158-159, 2004.
22. Xu, D. Q., Yang, W. L., Luo, S. P., Wang, B. T., Wu, J. and Xu, Z. Y. Fischer indole synthesis in Brønsted acidic ionic liquids: A green, mild, and regiospecific reaction system. *European Journal of Organic Chemistry*, 2007(6):1007-1012, 2007.
23. Xu, D. Q., Wu, J., Luo, S. P., Zhang, J. X., Wu, J. Y., Du, X. H. and Xu, Z. Y. Fischer indole synthesis catalyzed by novel SO_3H -functionalized ionic liquids in water. *Green Chemistry*, 11(8):1239-1246, 2009.
24. Li, B. L., Xu, D. Q. and Zhong, A. G. Novel SO_3H -functionalized ionic liquids catalyzed a simple, green and efficient procedure for Fischer indole synthesis in water under microwave irradiation. *Journal of Fluorine Chemistry*, 144:45-50, 2012.
25. Yi, F. P., Sun, H. Y., Pan, X. H., Xu, Y. and Li, J. Z. Synthesis of Fischer indole derivatives using carboxyl-functionalized ionic liquid as an efficient and recyclable catalyst. *Chinese Chemical Letters*, 20(3):275-278, 2009.
26. Kumar, T. O. S. and Mahadevan, K. M. Green synthesis of 2, 3, 4, 9-tetrahydro-1H-carbazoles/2, 3-dimethylindoles catalyzed by [bmim(BF_4)] ionic liquid in methanol. *Organic Communications*, 6(1):31-40, 2013.

27. Librando, I. L. and Creencia, E. C. Microwave-assisted Fischer indole synthesis of 1, 2, 3, 4-tetrahydrocarbazole catalyzed by 1, 3-dialkylimidazolium bromide ionic liquids. *Procedia Chemistry*, 16:299-305, 2015.
28. Hu, Y. L., Fang, D. and Li, D. S. Novel and efficient heterogeneous 4-methylbenzenesulfonic acid-based ionic liquid supported on silica gel for greener Fischer indole synthesis. *Catalysis Letters*, 146(5):968-976, 2016.
29. Neuhaus, W. C., Bakanas, I. J., Lizza, J. R., Boon, C. T. and Moura-Letts, G. Novel biodegradable protonic ionic liquid for the Fischer indole synthesis reaction. *Green Chemistry Letters and Reviews*, 9(1):39-43, 2016.
30. Ghumro, S. A., Saleem, S., al-Rashida, M., Iqbal, N., Alharthy, R. D., Ahmed, S., Moin, S. T. and Hameed, A. N, N-Dimethylpyridin-4-amine (DMAP) based ionic liquids: Evaluation of physical properties via molecular dynamics simulations and application as a catalyst for Fisher indole and 1 H-tetrazole synthesis. *RSC Advances*, 7(54):34197-34207, 2017.
31. Yu, J., Xu, J., Yu, Z., Jin, Y., Li, J. and Lv, Y. A continuous-flow Fischer indole synthesis of 3-methylindole in an ionic liquid. *Journal of Flow Chemistry*, 7(2):33-36, 2017.
32. Fan, W., Li, R., Ma, J., Fan, B. and Cao, J. Synthesis, characterization and catalytic properties of MFI-type zeolites prepared in the system $\text{Na}_2\text{O SiO}_2 \text{ Al}_2\text{O}_3 \text{ H}_2\text{N}(\text{CH}_2)_6\text{NH}_2 \text{ NH}_4\text{F}$. *Microporous Materials*, 4(4):301-307, 1995.
33. Jacobs, P. A., Beyer, H. K. and Valyon, J. Properties of the end members in the Pentasil-family of zeolites: Characterization as adsorbents. *Zeolites*, 1(3):161-168, 1981.
34. Jansen, J. C., Van der Gaag, F. J. and Van Bekkum, H. Identification of ZSM-type and other 5-ring containing zeolites by IR spectroscopy. *Zeolites*, 4(4):369-372, 1984.
35. Coudurier, G., Naccache, C. and Vedrine, J. C. Uses of IR spectroscopy in identifying ZSM zeolite structure. *Journal of the Chemical Society, Chemical Communications*, 24:1413-1415, 1982.
36. Zhang, Y., Zhou, Y., Huang, L., Xue, M. and Zhang, S. Sn-modified ZSM-5 as support for platinum catalyst in propane dehydrogenation. *Industrial & Engineering Chemistry Research*, 50(13):7896-7902, 2011.

37. Khatamian, M. and Irani, M. Preparation and characterization of nanosized ZSM-5 zeolite using kaolin and investigation of kaolin content, crystallization time and temperature changes on the size and crystallinity of products. *Journal of the Iranian Chemical Society*, 6(1):187-194, 2009.
38. Fan, F., Sun, K., Feng, Z., Xia, H., Han, B., Lian, Y., Ying, P. and Li, C. From molecular fragments to crystals: A UV Raman spectroscopic study on the mechanism of Fe-ZSM-5 synthesis. *Chemistry-A European Journal*, 15(13):3268-3276, 2009.
39. Yang, Y. L. and Kou, Y. Determination of the Lewis acidity of ionic liquids by means of an IR spectroscopic probe. *Chemical Communications*, 2:226-227, 2004.
40. Thommes, M., Kaneko, K., Neimark, A. V., Olivier, J. P., Rodriguez-Reinoso, F., Rouquerol, J. and Sing, K. S. Physisorption of gases, with special reference to the evaluation of surface area and pore size distribution (IUPAC Technical Report). *Pure and Applied Chemistry*, 87(9-10):1051-1069, 2015.
41. Vafi, L. and Karimzadeh, R. A novel method for enhancing the stability of ZSM-5 zeolites used for catalytic cracking of LPG: Catalyst modification by dealumination and subsequent silicon loading. *Chinese Journal of Catalysis*, 37(4):628-635, 2016.
42. Kore, R., Srivastava, R. and Satpati, B. ZSM-5 zeolite nanosheets with improved catalytic activity synthesized using a new class of structure-directing agents. *Chemistry-A European Journal*, 20(36):11511-11521, 2014.
43. Voogd, P., Scholten, J. J. F. and Van Bekkum, H. Use of the t-plot—De Boer method in pore volume determinations of ZSM-5 type zeolites. *Colloids and Surfaces*, 55:163-171, 1991.
44. Bhattacharya, D., Gammon, D. W. and Van Steen, E. Synthesis of 1, 2, 3, 4-tetrahydrocarbazole over zeolite catalysts. *Catalysis Letters*, 61(1-2):93-97, 1999.